Dynamical Identification of the Cooling System in a Fluidized Bed Combustor

Havlíček, A; Gustavsson, Ivar

1978

Document Version:
Publisher's PDF, also known as Version of record

CODEN: LUTFD2/(TFRT-7153)/1-067/(1978)

DYNAMICAL IDENTIFICATION OF THE COOLING SYSTEM IN A FLUIDIZED BED COMBUSTOR

A. HAVLÍČEK
I. GUSTAVSSON

Department of Automatic Control
Lund Institute of Technology
October 1978

Dokumentutgivare
Lund Institute of Technology
Handläggare
Department of Automatic Control
I Gustavsson

Dokumentnamn
REPORT

Utgivningsdatum
Oct 1978

Dokumentbeteckning
LUTFD2/(TFRT-7153)/1-67/(1978)

Ärendebeteckning

Författare
A Havlíček
I Gustavsson

Dokumenttitel och undertitel

DYNAMICAL IDENTIFICATION OF THE COOLING SYSTEM IN A FLUIDIZED BED COMBUSTOR

Referat (sammandrag)

Experimental identification of the cooling system in a fluidized bed combustor pilot-scale unit installed at the Institute of Chemical Process Fundamentals in Prague has been performed. The main objective of the study was to obtain the information necessary for designing a controller for the system, possibly using adaptive control. As the mechanism of the cooling system is rather complex, the method chosen was the only way to get realistic information. Modelling using physical analysis is extremely difficult. The data were processed at the Department of Automatic Control, Lund Institute of Technology using the interactive identification program package IDPAC. A first order dynamical model has been found to be adequate.

Referat skrivet av
Authors

Förslag till ytterligare nyckelord

Klassifikationssystem och -klass(er)

Indextermer (ange källa)

Omfång
67 pages

Övriga bibliografiska uppgifter

Språk
English

Sekretessuppgifter

ISSN

ISBN

Dokumentet kan erhållas från
Department of Automatic Control
Lund Institute of Technology
Box 725, S-220 07 LUND 7, Sweden

Mottagarens uppgifter

Pris

DYNAMICAL IDENTIFICATION OF THE COOLING SYSTEM IN A FLUIDIZED BED COMBUSTOR

by

A. Havlíček
Czechoslovak Acad. Sci.
Inst. Chem. Proc. Fundamentals

and

I. Gustavsson
Lund Institute of Technology
Department of Automatic Control

TABLE OF CONTENTS

1. INTRODUCTION

This report discusses the dynamical identification of a new cooling system for the fluidized bed combustor, which was described in Beránek (1975). The combustion of bad quality coal or waste oil is running simultaneously with the sulphur removal process based on the reaction between SO_2 and certain additive particles. The additive particles are usually of limestone, dolomite or lime, which are fed into the fluidized bed. The new method for the heat removal from the fluidized bed combustor makes it possible to maintain a constant temperature of the fluidized bed, not only with various types of coal but also with various feeding rates of fuel. This method for a continuous control of the temperature in the fluidized bed combustor is based on the immersion of the heat exchanger in the lower part of the fluidized bed, and on the supply of the air needed, partly below the heat exchanger, partly at the top of it. By changing the ratio of the air flow delivered under the exchanger and above it, the amount of heat being transfered from the fluidized bed by the boiling water flowing through the heat exchanger can be varied over a wide range.

The efficiency of sulphur removal from the flue gas is strongly dependent on the temperature in the fluidized bed. A comparison of the temperature dependence on the sulphur removal efficiency for different species of limestone and dolomites is shown in Fig. 1. It is obvious that the temperature for the

optimal sulphur removal lies in a very narrow temperature interval. It follows from the previous descussion that a good quality control is necessary. In particular, it seems reasonable to use adaptive control to be able to maintain an optimal point in the temperature for the sulphur removal process. It is therefore important to have a good enough dynamical description of the whole process. A first step towards this is to model the cooling system dynamically.

2. EXPERIMENTAL SET-UP AND MEASUREMENT TECHNIQUES

The experimental equipment for the fluidized bed combustor is schematically represented in Fig. 2, see also Beránek (1975). The fluidized bed reactor is constructed from heat-resistant steel POLDI-AKX. The cross-section of the lower part of the reactor is 0.3 x 0.3 m. The height of the reactor is 1.7 m. The upper part of the reactor which accomodates the thermometers, sockets for the flue gas outlets measuring and withdrawing of bed samples is extended to 0.6 x 0.6 m. The bottom of the reactor is constituted from three sections of caps, symmetrically distributed over the cross-section of the reactor. Two sections are for air supply and the third one for town gas which is used for warming up the reactor. By dividing the air flow into two streams and by their distribution into different levels of the fluidized bed a continuous control of the heat transfer from the fluidized bed may be achieved. A heat exchanger is located in the volume between the two air inlets into the bed, Beránek et al (1970) (see Fig. 2, inlets 1 and 2).

The temperature of the fluidized bed is maintained at the requested value by means of a pneumatic regulator. The input signal for the regulator is the voltage of the thermocouple Pt-PtRh located approximately in the middle of the fluidized bed. Two pneumatic valves (5 and 6 in Fig. 2) are being controlled by the outlet pressure from the pneumatic regulator. One of the valves is closing, the other one is opening with

increasing pressure. The control of the temperature of the fluidized bed can be maintained in this way independently of the calorific value of the fuel fed into the fluidized bed.

A scheme of the measurement equipment is shown in Fig. 3. The thermocouple Pt-PtRh which is located in the middle of the fluidized bed produces a voltage signal which is linearly dependent on the temperature in the working range. An amplifier normalizes the signal so that 1 mV corresponds to 1^{o}C. The temperature signal is measured (mV signal) directly by the data acquisition system which is composed of a digital voltmeter and a scanner. The signal is punched on a paper tape in ASCII code after the A/D conversion. The temperature signal is considered as the output signal of the system. The input signal is the measured pressure at the input of the pneumatic valves. The pressure is measured by means of a piezoelectric pressure sensor. The voltage signal from the sensor is amplified and connected to the first channel of the data acquisition system and punched on a paper tape. The calibration curve for the voltage dependence on the pressure is given in Fig. 4. The curve is exactly linear. The time delay between the measurements of the two channels is about 10 ms, which is not important compared to the sampling interval used (see below).

3. DESCRIPTION OF THE EXPERIMENTS

Four experiments were performed on the fluidized bed combustor at the Institute of Chemical Process Fundamentals - Prague 6. A summary of the essential parameters of the experiments is given in Table 1. The choice of sampling interval and length of one pulse of the input signal was based on preliminary experiments. The sampling interval of 1 or 2 s was chosen because of the contents of frequencies in the interval 0 - 0.1 Hz in the output signal of the system. The time constant of the system was estimated roughly to 120 s. The length of the pulse for the step response experiment was therefore chosen as 150 s. The length of one pulse for the pseudorandom binary signal (PRBS) experiments was chosen as 20 or 40 s. The experiments 2-4 lasted one period of the PRBS signal (31 pulses). The system was roughly in steady state in the working point corresponding to the average value of the input signal. The experiments 2 and 3 (Figs. 6b and 7b) are, however, a little away from this point because the measurements are made with the system in open loop without any regulator. Then there were some troubles holding the system in the stationary regime. The input signal was generated by hand turning a pneumatic valve using a table of the PRBS sequence. The input and output signals of the experiments 1-4 are shown in Figs. 5-8 with the input signal in part a and the output signal in part b of each figure.

Exp No	Sample interval in s	No of points	Duration of exp. in s	Input signal	Length of one pulse in s
1	1	800	800	steps	150
2	1	770	770	PRBS	20
3	2	740	1480	PRBS	40
4	2	370	740	PRBS	20

Table 1 Characteristics of the experiments performed

4. DATA ANALYSIS

An interactive identification program package IDPAC used at the Lund Institute of Technology and described in Wieslander (1976) was used for the data analysis. The program was run on a control computer (PDP-15). To illustrate the use of the package an example of a sequence of commands which was used for the identification of the first experiment is given.

Example.

```
MOVE DK EXP1←DT EXP1                    1)
ML MLE11←EXP1 1                         2)
PRINT MLE11                             3)
RESID RDE11←MLE11 EXP1 20               4)
DETER D11←MLE11 EXP1(1)                 5)
PLOT 800 EXP1(2) D11                    6)
```

1) This commands initiates the transfer of the input and output vectors of the first experiment (EXP1(1) and EXP1(2)) from a magnetic tape to the disc.
2) The parameters of a first order difference equation model (MLE11) are estimated using the maximum likelihood method, see below.
3) The resulting model MLE11 is printed on the line-printer.
4) The residuals of the model are tested by different statistical tests and put into the data file RDE11.
5) The output (D11) of the deterministic part of the model

is computed using the input of the experiment (EXP1(1)) as input.

6) The measured output (EXP1(2)) and the deterministic model output (D11) are plotted on the display.

The commands 2)-6) are then repeated for models of order 2 and 3.

The maximum likelihood method, Åström and Bohlin (1965) and Gustavsson (1969) is used for the identification of linear, single output, time invariant, discrete-time stochastic systems of the form

$$A(q^{-1})y(t) = B(q^{-1})u(t) + \lambda C(q^{-1})e(t) \qquad (4.1)$$

where u(t) is the input, y(t) the output and e(t) a sequence of independent normal (0,1) random variables. The variable e(t) is assumed to be independent of the input u(t). The forward shift operator is denoted by q. The polynomials $A(q^{-1})$, $B(q^{-1})$ and $C(q^{-1})$ are defined by

$$\begin{aligned} A(q^{-1}) &= 1 + a_1 q^{-1} + \ldots + a_n q^{-n} \\ B(q^{-1}) &= b_1 q^{-1} + \ldots + b_n q^{-n} \\ C(q^{-1}) &= 1 + c_1 q^{-1} + \ldots + c_n q^{-n} \end{aligned} \qquad (4.2)$$

where n is the order of the system. The negative logarithm of the likelihood function has the form

$$-\ln L(\theta,\lambda) = \frac{1}{2\lambda^2}\sum_{1}^{N}\varepsilon^2(t) + N \ln \lambda + \frac{N}{2}\ln 2\pi \qquad (4.3)$$

for the given record of input-output data, u(t) and y(t), of length N. $\varepsilon(t)$ are the residuals defined recursively by

$$C(q^{-1})\varepsilon(t) = A(q^{-1})y(t) - B(q^{-1})u(t) \qquad (4.4)$$

The likelihood function is considered as a function of θ and λ, where θ is a vector with the components $(a_1,\ldots,a_n,b_1,\ldots,b_n,c_1,\ldots,c_n)$. The maximization of the likelihood function $L(\theta,\lambda)$ can be performed separately with respect to θ and λ. According to Åström and Bohlin (1965) the maximum of $L(\theta,\lambda)$ is obtained by finding θ which minimizes

$$V(\theta) = \frac{1}{2}\sum_{1}^{N}\varepsilon^2(t) \qquad (4.5)$$

The estimation problem is thus equivalent to minimizing a function of several variables. To test if the reduction of the loss function is significant when the order of the model (4.1) is increased from n to m the following test quantity can be used

$$t_{m,n} = \frac{V_n - V_m}{V_m} \cdot \frac{N - k_m}{k_m - k_n} \qquad m > n \qquad (4.6)$$

where V_n is the minimum value of the loss function for a model or order n, N is the number of input-output pairs and k_n is the number of parameters in a model of n-th order. It can be shown that the random variable $t_{m,n}$ has an $F(N-k_m, k_m-k_n)$ distribution for large n. The null hypothesis:

$$H_0: a_{n+1} = \ldots = a_m = b_{n+1} = \ldots = b_m = c_{n+1} = \ldots = c_m = 0 \qquad (4.7)$$

At a risk level of 5 % we have F(100,3) = 2.6.

Another test for determining the order of the model is the so called Akaike´s information criterion, Akaike (1972), where a test quantity AIC of the form

$$AIC = N\,(1 + \ln 2\pi + 2 \ln \hat{\lambda}) + 2\,k_n \qquad (4.8)$$

is computed where $\hat{\lambda}$ is the estimated standard deviation of the residuals. The variable AIC should have a minimum for the correct order of the model according to Akaike.

Using the model described by equation (4.1) we get directly a description of the disturbances together with the input-output model in the form

$$y_D(t) = \lambda C(q^{-1})/A(q^{-1})e(t) \qquad (4.9)$$

If the disturbances of the process are measured, i.e. without exciting the process with any input signals, it is possible to model them directly by a model of the form (4.9). This can be done using the available program package. To illustrate this we have subtracted the deterministic model output from the measured output and then identified the remaining part of the signal which can be considered as the total disturbance acting on the process.

5. IDENTIFICATION RESULTS

In this section the identification results for the four experiments will be presented. In the first part we consider the identification of the whole data sets including the beginning of the data series where some form of transient behaviour can be observed. In the second part the first 100 points of the experiments were excluded so that the process approximately has reached a stationary behaviour. In both cases models up to the third order were identified from the data. The maximum value of three was chosen partly from physical point of view and partly from the results of the statistical model order tests. The physical process consists of transfer between input pressure and the moving of the valves (simultaneous opening and closing the valves 5 and 6) which results in increasing or decreasing the cooling intensity followed by the bed temperature changes.

In Table 2 the results from the identification of the whole data sets are presented. The models are denoted by MLEij where i is the number of the experiment and j the order of the model. The parameters of the models, the obtained loss function values and the value of the Akaike´s information criterion are given. The loss function is decreasing with increasing order of the model. The AIC value has its minimum for the first order models except for the third experiment where a second order model is indicated. The test quantity given by equation (4.6) is computed. Let us assume the null hypothesis

Model	n	Δt	a_1	a_2	a_3	b_1	b_2	b_3	c_1	c_2	c_3	λ	V	AIC
MLE11	1	1	-0.990	-	-	-6.13	-	-	-0.898	-	-	5.815	13527	4293.1
MLE12	2	1	-0.507	-0.478	-	3.60	-12.7	-	-0.381	-0.470	-	5.810	13502	4297.6
MLE13	3	1	-0.509	-0.102	-0.369	2.15	6.76	-20.5	-0.390	-0.114	-0.300	5.804	13475	4302.0
MLE21	1	1	-0.991	-	-	-4.54	-	-	-0.851	-	-	5.783	12876	4124.0
MLE22	2	1	-1.190	0.198	-	-7.11	3.51	-	-1.090	0.216	-	5.776	12846	4128.0
MLE23	3	1	-0.395	-0.748	0.157	-18.1	20.0	-8.50	-0.293	-0.657	0.178	5.775	12840	4133.6
MLE31	1	2	-0.984	-	-	-9.51	-	-	-0.791	-	-	6.220	14309	4070.8
MLE32	3	2	-0.076	-0.900	-	-44.3	26.8	-	0.118	-0.748	-	6.190	14177	4070.0
MLE33	3	2	0.082	-0.115	-0.923	-38.1	15.4	-5.73	0.267	0.073	-0.730	6.186	14159	4075.0
MLE41	1	2	-0.980	-	-	-9.74	-	-	-0.904	-	-	5.582	5763.7	1958.4
MLE42	2	2	-0.146	-0.815	-	-5.96	-12.0	-	-0.084	-0.734	-	5.580	5757.7	1964.0
MLE43	3	2	-1.730	1.156	-0.416	21.9	-61.4	33.7	-1.660	1.120	-0.400	5.530	5651.0	1963.0

Table 2 Results from the identification of the whole data sets

$$a_2 = b_2 = c_2 = 0 \qquad (5.1)$$

The test quantities $t_{2,1}$ for the different experiments are

Exp 1: 0.49

Exp 2: 0.595

Exp 3: 2.278

Exp 4: 0.13

If we then use a risk level of 5 % which corresponds to a value of the test quantity of 2.6 (for N $\geq$ 100) we find that for all our experiments the loss function is not reduced significantly when increasing the order from one to two. The null hypothesis is therefore accepted.

For illustration purposes we present in Figs. 9-12 the autocorrelation functions of the residuals and the crosscorrelation functions between the residuals and the input signals for all four experiments for the models of the first order. In part a) of the figures the autocorrelation function is shown and in part b) the corresponding crosscorrelation function. There is no value of the autocorrelation functions outside the $\pm$ 2δ limit which means that we can accept that the residuals are white. We get similar information from the crosscorrelation functions. It is possible to conclude that there is no correlation between the residuals and the input. This again indicates that a first order model is sufficient.

In Figs. 13-16 there is a comparison between the measured

outputs and the deterministic model outputs for the different experiments. We observe that for the experiments 2 and 3 there is a large discrepancy between the two signals in the beginning of the experiments (approximately 100 points). This can be explained as a transient in the output signal caused by the fact the process was operating at a point different from the average value of the input signal.

The results can be summarized in the following models

$$\text{Exp 1:}\quad y(t) = \frac{-6.13q^{-1}}{1-0.990q^{-1}}u(t) + 5.82\,\frac{1-0.898q^{-1}}{1-0.990q^{-1}}e(t) \qquad (5.2)$$

$$\text{Exp 2:}\quad y(t) = \frac{-4.54q^{-1}}{1-0.991q^{-1}}u(t) + 5.78\,\frac{1-0.851q^{-1}}{1-0.991q^{-1}}e(t) \qquad (5.3)$$

$$\text{Exp 3:}\quad y(t) = \frac{-9.51q^{-1}}{1-0.984q^{-1}}u(t) + 6.22\,\frac{1-0.791q^{-1}}{1-0.984q^{-1}}e(t) \qquad (5.4)$$

$$\text{Exp 4:}\quad y(t) = \frac{-9.74q^{-1}}{1-0.980q^{-1}}u(t) + 5.58\,\frac{1-0.904q^{-1}}{1-0.980q^{-1}}e(t) \qquad (5.5)$$

A first order discrete time system $bq^{-1}/(1-aq^{-1})$ can be considered as the result of sampling a continuous system $K/(1+sT)$ assuming that the input signal is constant between the sampling events. We have $a = e^{-\Delta T/T}$ and $b = K(1-e^{-\Delta T/T})$, where ΔT is the sampling interval. Calculating the time constant and the gain of the corresponding continuous models to (5.2) - (5.5) we get the results shown in Table 3.

	MLE11	MLE21	MLE31	MLE41
ΔT (s)	1	1	2	2
T (s)	104	108	124	99
K	635	491	590	582

Table 3

As a final check the amplitude and phase for the obtained models have been computed as well as the power spectrum of the disturbance part of the models. The results are shown in Figs. 19-21. There is a good agreement between all models except that the power of the disturbances is quite much lower in experiment 4, what indicates the beginning breakdown of the thermoelement.

Consider now what happens if we subtract the deterministic model output from the measured one which means that the remaining part of the signal is the disturbances acting on the process, and then identify this signal as a time series using the model (4.9). This identification is only made for the fourth experiment since there is only a small transient in this experiment. The identification is done using the following command sequence.

```
VECOP V41←EXP4(2)←D41          1)
ML M1V41←V41 1                 2)
RESID R1V41←M1V41 V41 20       3)
```

1) The deterministic model output D41 is subtracted from the measured one (EXP4(2)). The model output D41 is obtained from the first order model.
2) A first order model of the form (4.9) is estimated using the maximum likelihood method.
3) The residuals are computed and put into the data file R1V41 and different statistical tests of them are provided.

The steps 2)-3) are then repeated for orders 2-4 of the model. The results of the identification are given in Table 4. A plot of the residuals for the first order model is shown in Fig. 17. The AIC value is minimum for the first order model. The value of $t_{2,1} = 0.36$ also indicates that a first order model is sufficient. The autocorrelation function of the residuals is shown in Fig. 18, which also supports the choice of the first order model. The following model is accepted

$$y_D(t) = 5.57 \frac{1-0.869q^{-1}}{1-0.950q^{-1}} e(t) \qquad (5.6)$$

This model compares well with the second part of the model (5.5). The discrepancy is explained by the fact that when estimating a model of the structure (5.5) the parameter a_1 is common to the deterministic and stochastic parts of the model. If we instead use the approach here this coupling does not exist. A more straightforward way would be to have different denominators for the deterministic and stochastic parts of the model, in the first place.

	M1V41	M2V41	M2V41	M4V41
n	1	2	3	4
ΔT	2	2	2	2
a_1	-0.950	-1.93	-2.13	-0.083
a_2		0.835	1.317	-0.402
a_3			-0.187	-0.610
a_4				0.205
c_1	-0.869	-1.867	-2.05	0.003
c_2		0.877	1.217	-0.330
c_3			-0.159	-0.631
c_4				0.247
λ	5.571	5.56	5.56	5.540
V	5740.8	5723.3	5721.7	5678.6
AIC	1955.0	1957.8	1961.7	1962.9

Table 4

We will now study if the transient found especially in the experiments 2 and 3 has any substantial influence on the models. To do so the first 100 data of the data series have been disregarded for all the four experiments. The obtained results are presented in Table 5 where the models are denoted MLCij. For these models we get

EXP1: $t_{2,1} = 1.727$

EXP2: $t_{2,1} = 0.619$

Model	n	Δt	a_1	a_2	a_3	b_1	b_2	b_3	c_1	c_2	c_3	λ	V	AIC
MLC11	1	1	-0.989	-	-	-5.64	-	-	-0.865	-	-	5.854	12010	3771.8
MLC12	2	1	-0.774	-0.209	-	66.7	-73.9	-	-0.614	-0.226	-	5.832	11921	3772.6
MLC13	3	1	-0.677	0.409	-0.702	91.9	-80.9	-22.9	-0.512	0.382	-0.595	5.813	11845	3774.1
MLC21	1	1	-0.991	-	-	-4.42	-	-	-0.867	-	-	5.754	11109	3587.7
MLC22	2	1	-1.192	0.199	-	-5.31	1.77	-	-1.112	0.227	-	5.746	11078	3591.7
MLC23	3	1	-0.939	-0.052	0.001	-14.2	17.9	-8.51	-0.859	-0.009	0.020	5.746	11075	3597.6
MLC31	1	2	-0.981	-	-	-8.54	-	-	-0.811	-	-	6.206	12325	3518.9
MLC32	2	2	-1.018	0.033	-	-17.3	9.22	-	-0.844	0.017	-	6.202	12310	3524.1
MLC33	3	2	0.069	-0.038	-0.975	-24.7	8.71	-10.1	0.238	0.159	-0.806	6.134	12040	3515.9
MLC41	1	2	-0.985	-	-	-9.67	-	-	-0.946	-	-	5.636	4258.4	1438.4
MLC42	1	2	-0.003	-0.968	-	-14.5	-4.48	-	0.043	-0.942	-	5.600	4248.1	1443.7
MLC43	3	2	-1.383	0.382	0.008	38.9	-101.1	57.1	-1.387	0.453	-0.066	5.475	4062.7	1437.6

Table 5

EXP3: $t_{2,1} = 0.258$

EXP4: $t_{2,1} = 0.213$

The AIC quantity has its minimum value for the first order model for the experiments 1 and 2 and for the third order model for the experiments 3 and 4. The autocorrelation functions for the residuals and the crosscorrelation functions between the residuals and the input signals are shown in Figs. 22-25. Based on this information it is possible to conclude that a first order model is acceptable for our purposes. In Figs. 26-27 there is a comparison between the deterministic model outputs and the measured outputs for experiments 2 and 3. The signals now have a better agreement in the beginning than when the transients were there.

The obtained models can be summarized as

$$\text{EXP1:}\quad y(t) = \frac{-5.64q^{-1}}{1-0.989q^{-1}}u(t) + 5.85\frac{1-0.865q^{-1}}{1-0.989q^{-1}}e(t) \qquad (5.7)$$

$$\text{EXP2:}\quad y(t) = \frac{-4.42q^{-1}}{1-0.991q^{-1}}u(t) + 5.75\frac{1-0.867q^{-1}}{1-0.991q^{-1}}e(t) \qquad (5.8)$$

$$\text{EXP3:}\quad y(t) = \frac{-8.54q^{-1}}{1-0.981q^{-1}}u(t) + 6.21\frac{1-0.811q^{-1}}{1-0.981q^{-1}}e(t) \qquad (5.9)$$

$$\text{EXP4:}\quad y(t) = \frac{-9.67q^{-1}}{1-0.985q^{-1}}u(t) + 5.61\frac{1-0.946q^{-1}}{1-0.985q^{-1}}e(t) \qquad (5.10)$$

In the Table 6 the gains and time constants of the corresponding continuous systems are given.

	MLC11	MLC21	MLC31	MLC41
Δt (s)	1	1	2	2
T (s)	92	113	105	129
K	516	501	507	623

Table 6

The transfer functions for the first order models of the four experiments are compared in Figs. 28-30. These curves are very much the same as was shown in Figs. 19-21 indicating that the initial transient part was without any large influence in this case.

6. CONCLUSIONS

The results of the identification of the four experiments show that a first order model well describes the dynamic behaviour of the process. The models of the different experiment as well as the models obtained with and without the initial transient in the data are almost similar. This confirms the conclusion that the obtained model is sensible. We have thus obtained a dynamical model of the cooling of the fluidized bed which in this case is a new system. This information can be used for the design of adaptive algorithms for the control of the sulphur removal process from the outlet gas of the reactor. Also we have obtained models of the disturbances acting on this process.

REFERENCES

1. Beránek J.: Sulphur removal during fluidized bed combustion, Paper presented at 5th International Congress CHISA´75, Prague 1975
2. Beránek J., Kašpar M., Bažant V., Chládek A.: Method for cooling or heating of fluidized bed, Czechoslovak patent No 148 943, 1970; U.S. patent No 1,395 078
3. Wieslander J.: IDPAC-User´s quide, Report 7605, April 1976, Department of Automatic Control, Lund Institute of Technology
4. Åström K.J., Bohlin T., Wensmark S.: Automatic construction of linear stochastic dynamic models for stationary processes with random disturbances using operating records, Report TP 18.150 (1965), IBM Nordic Laboratory, Sweden
5. Gustavsson I.: Parametric Identification of multiple input, single output linear dynamic systems, Report 6907 (1969), Dept. of Automatic Control, Lund Inst. of Techn. Lund, Sweden
6. Čermák J., Drahoš J., Havlíček A., Selucký K.: Application of Probability Modelling and Statistical Identification Method in Analysis of Fluidized Bed Combustion Reactor, Report 1978, ÚTZCHT ČSAV.

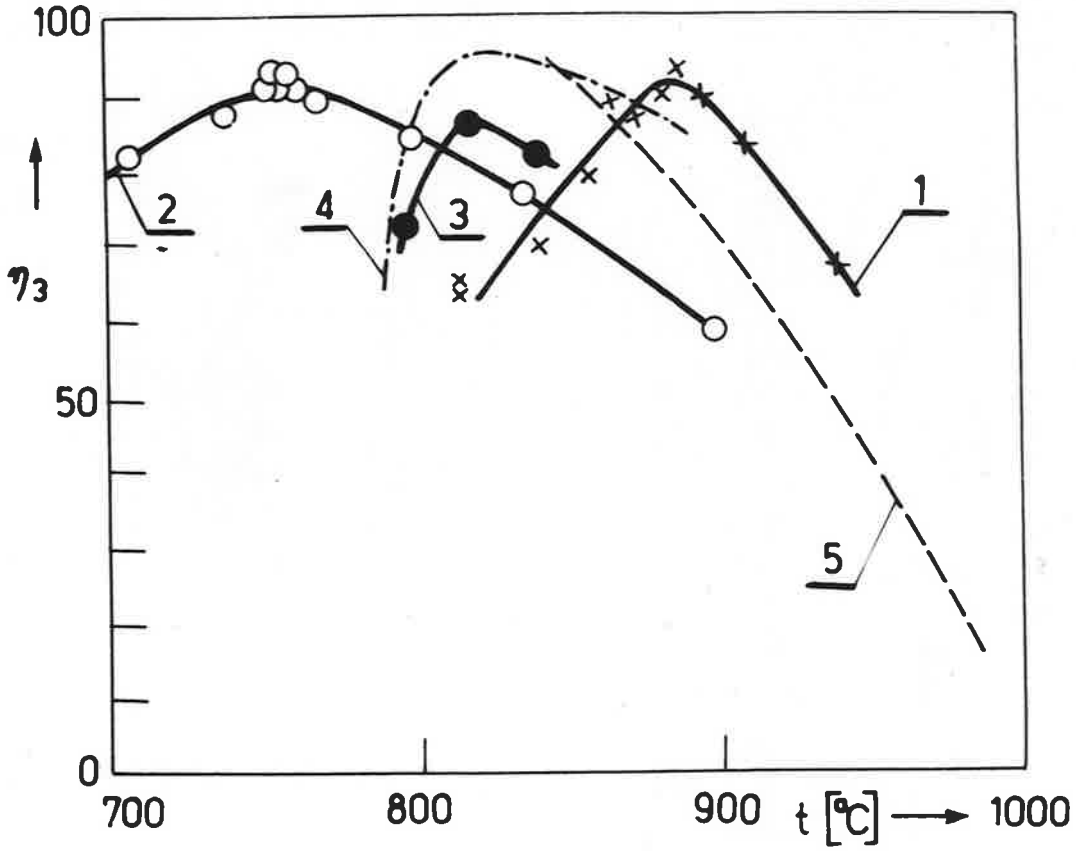

Fig. 1 Dependency of the desulphurization efficiency on the temperature and kind of additives

1 (crosses), Limestone Měrotín, 0.5-0.75 mm,

2 (empty circles), Dolomite Krty, 0.5-0.75 mm,

3 (full circles), Limestone Štramberk, 0.1-1 mm,

4 Limestone USA No. 1359[1)],

5 Dolomite USA No. 1337[1)].

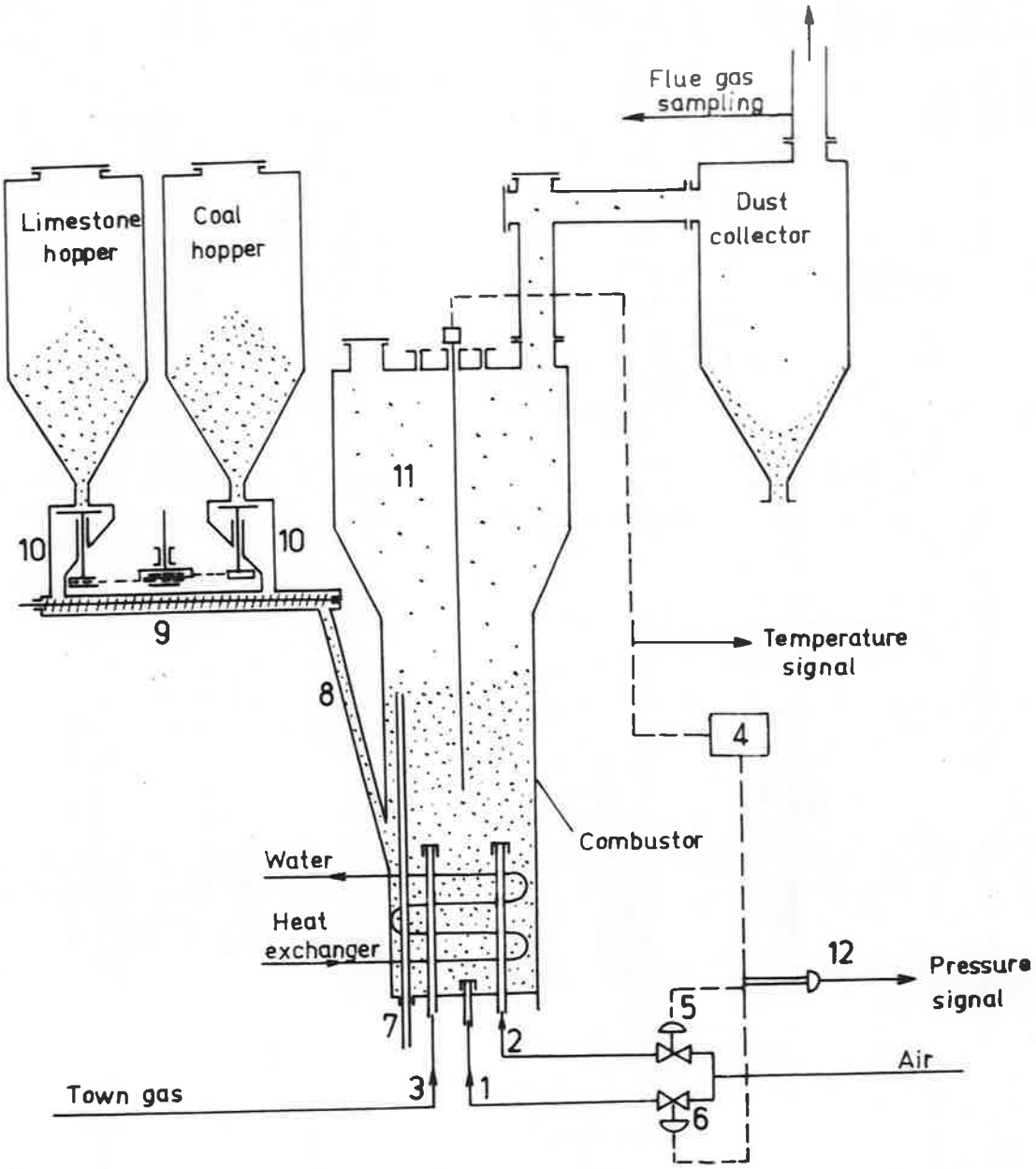

Fig. 2 Experimental equipment of Institute of Chemical Process Fundamentals

1,2 air inlet, 3 town gas inlet, 4 automatic temperature regulator, 5,6 pneumatic controlling valves, 7 overflow pipe, 8 downfall pipe, 9 screw conveyour, 10 plate feeder, 11 thermocouple, 12 pressure sensor

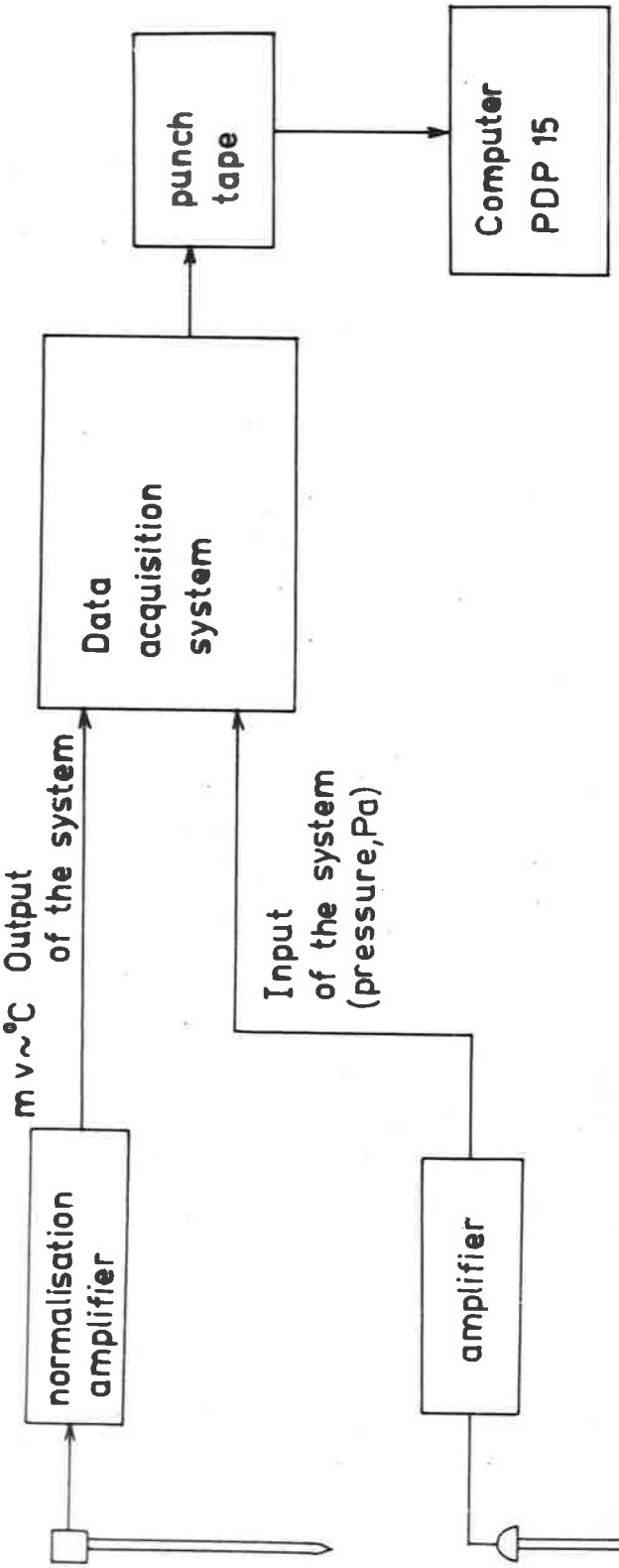

Fig. 3 Scheme of the measurement equipment

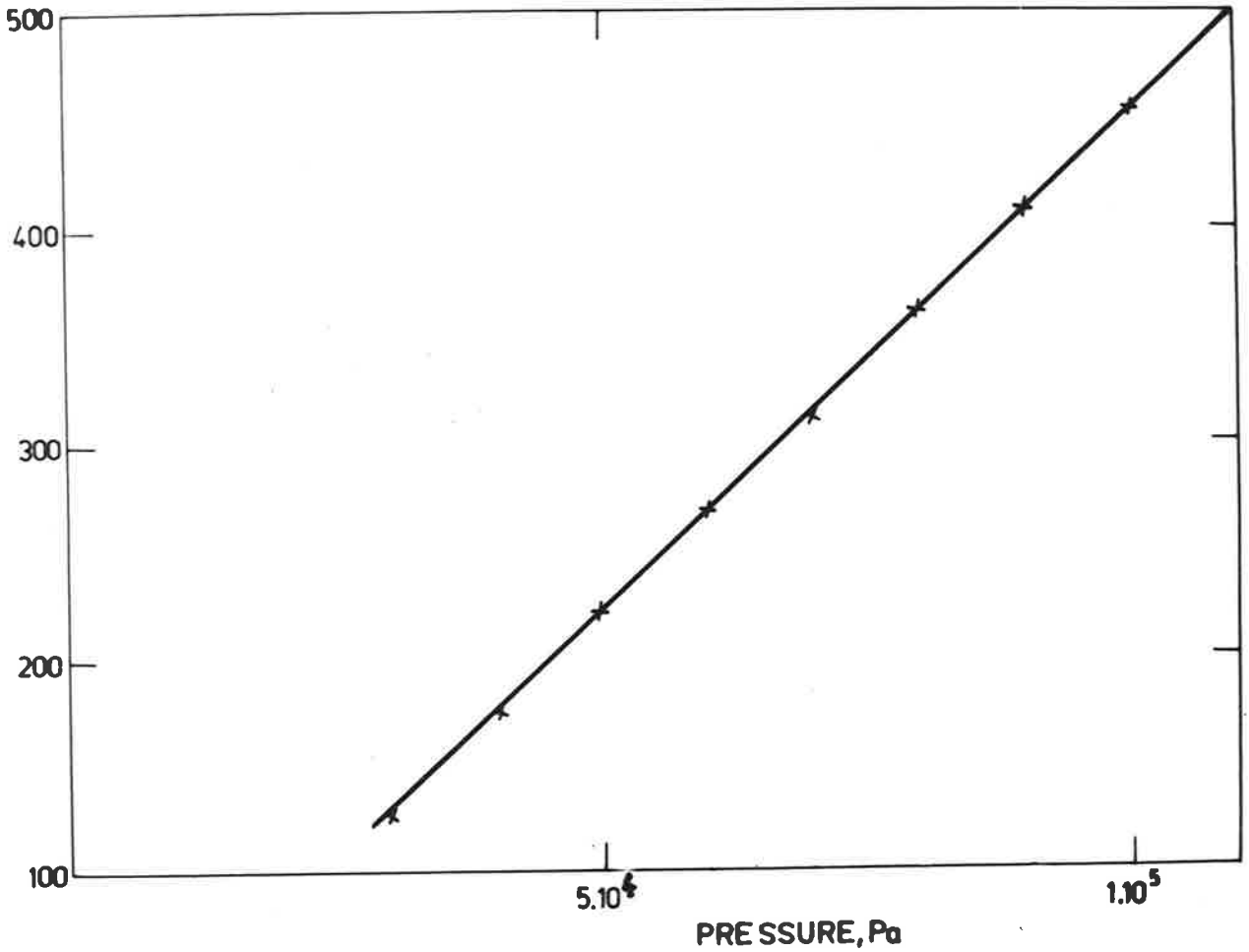

Fig. 4 The calibration curve for the voltage dependence on the pressure

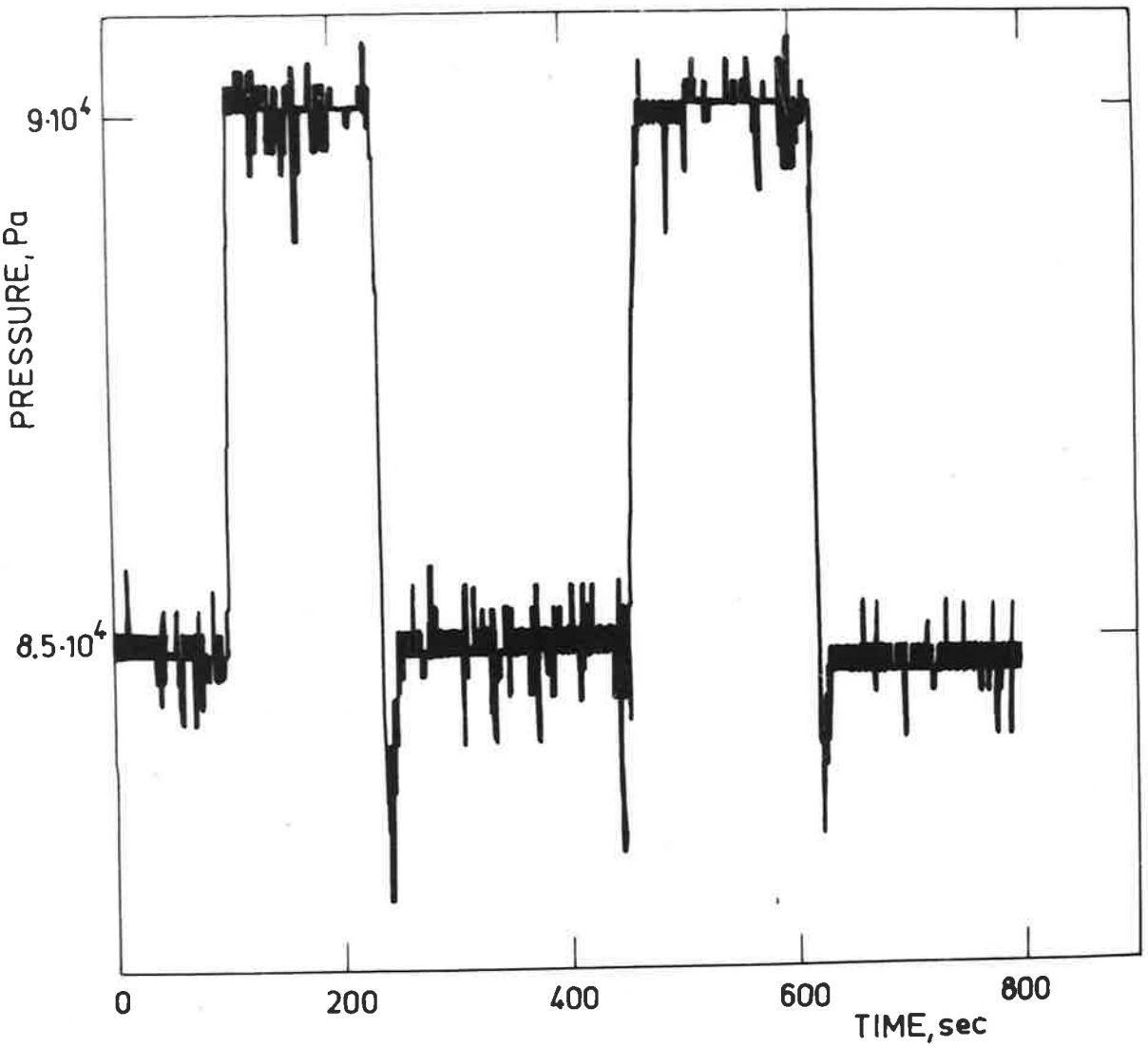

Fig. 5a Input signal of the exp. No. 1

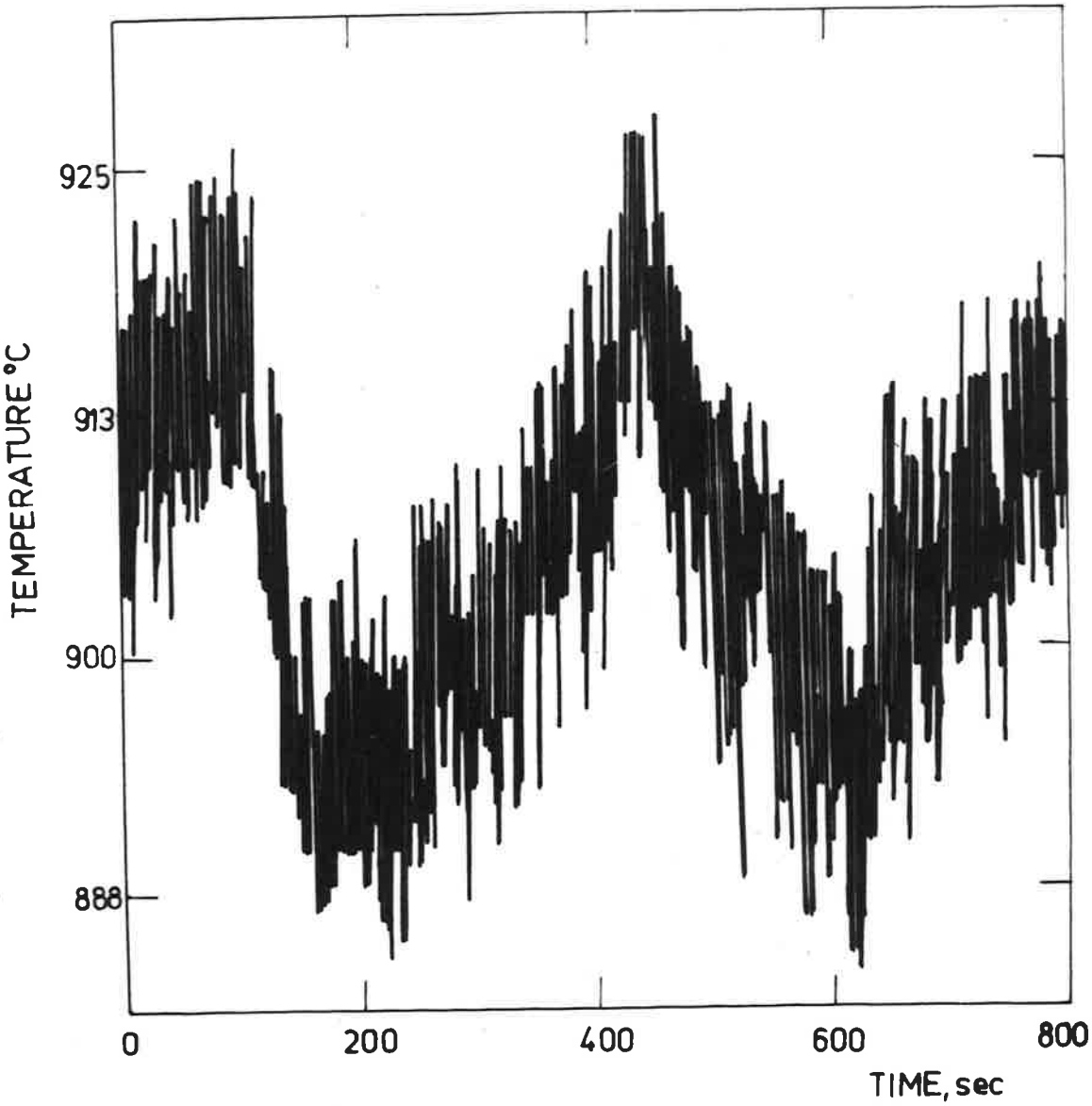

Fig. 5b Output signal of the exp. No. 1

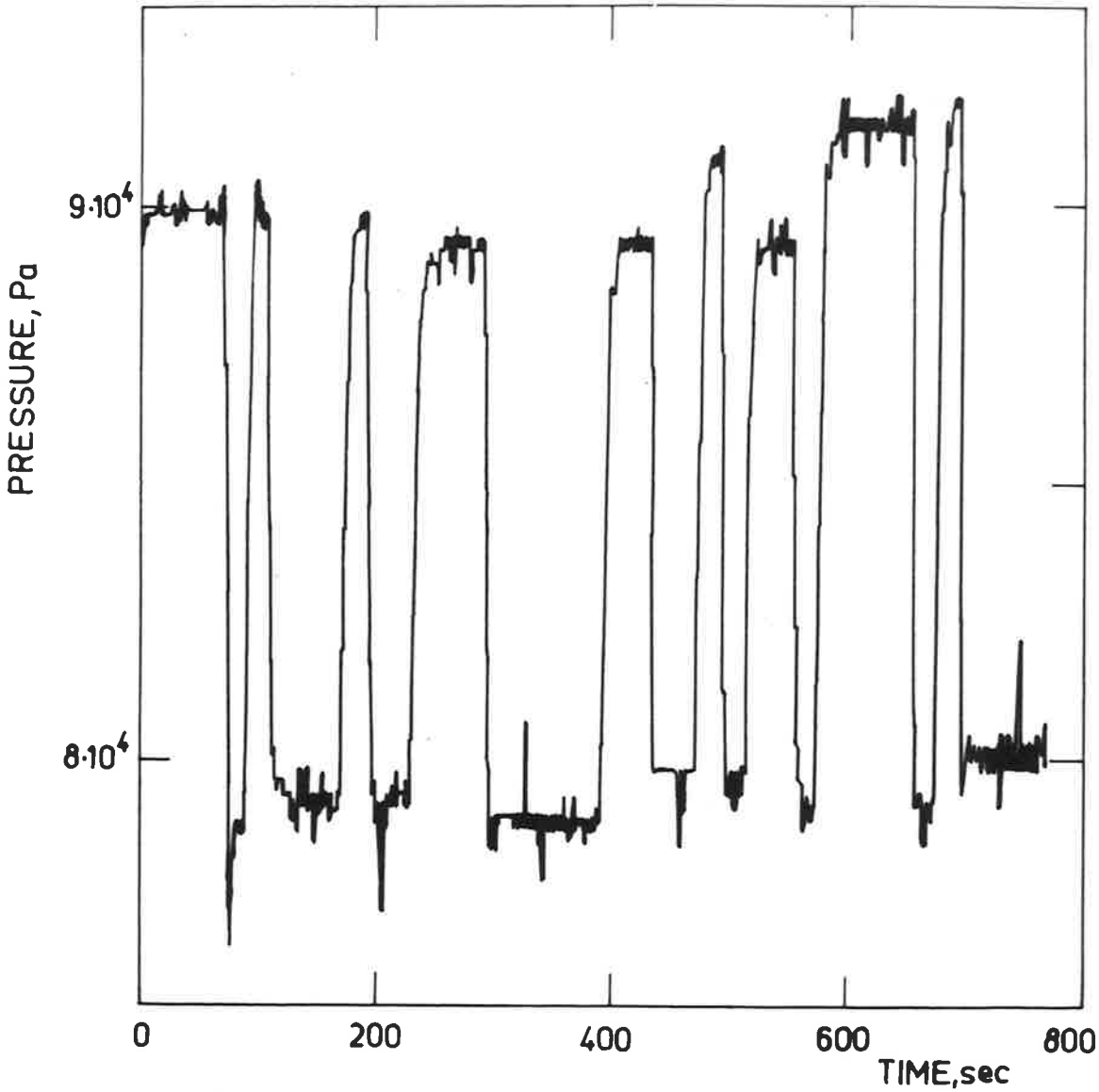

Fig. 6a Input signal of the exp. No. 2

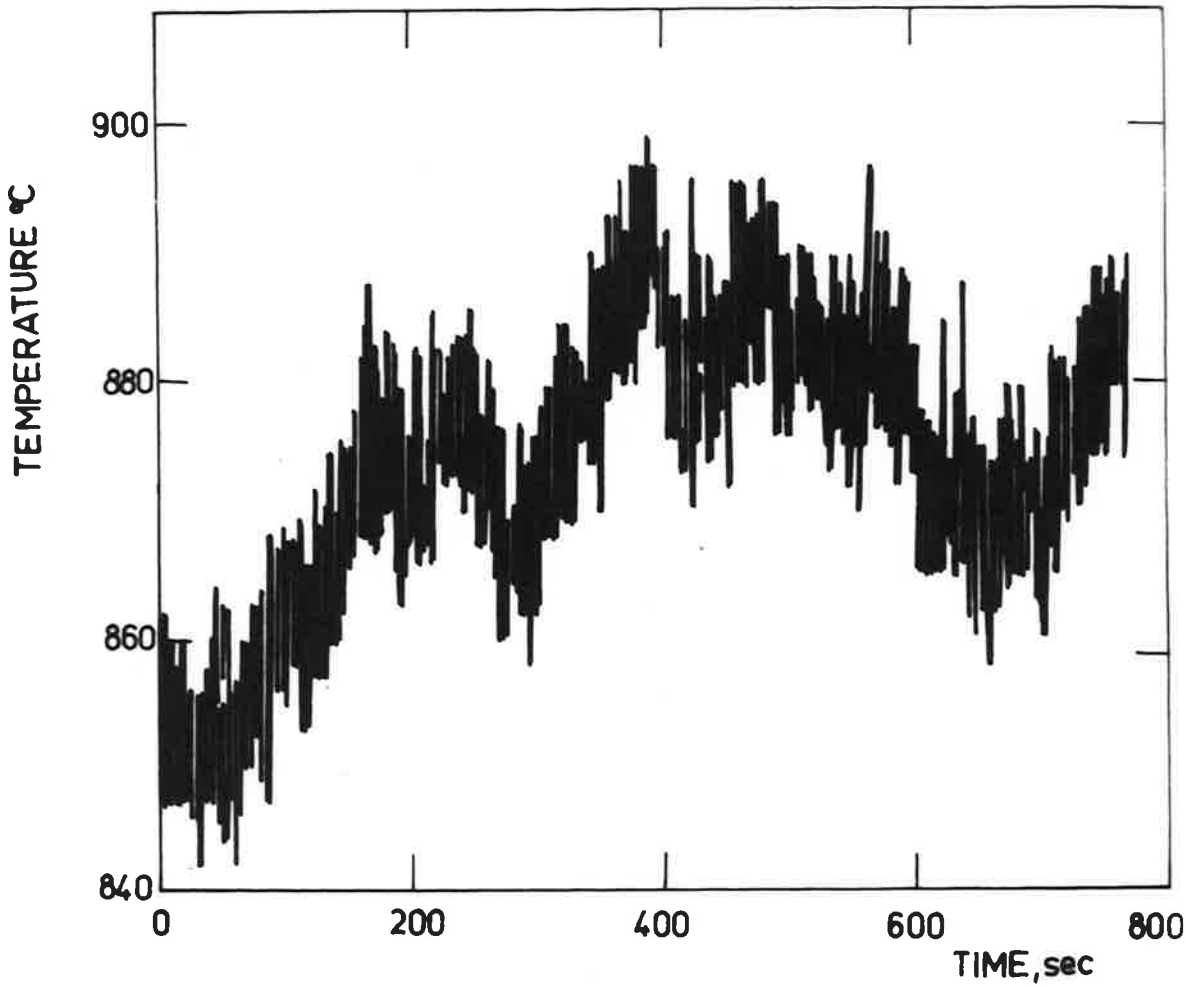

Fig. 6b Output signal of the exp. No. 2

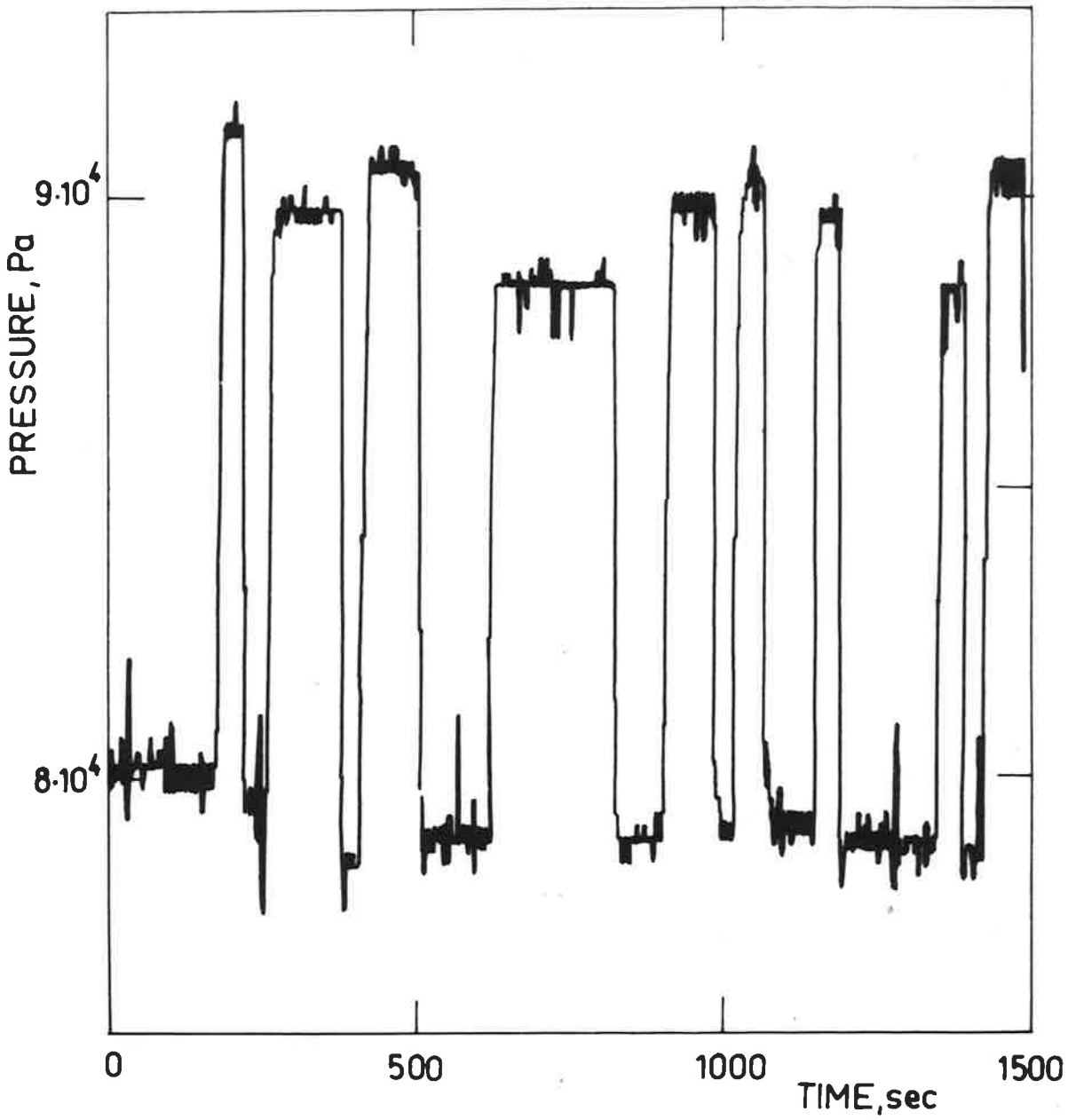

Fig. 7a Input signal of the exp. No. 3

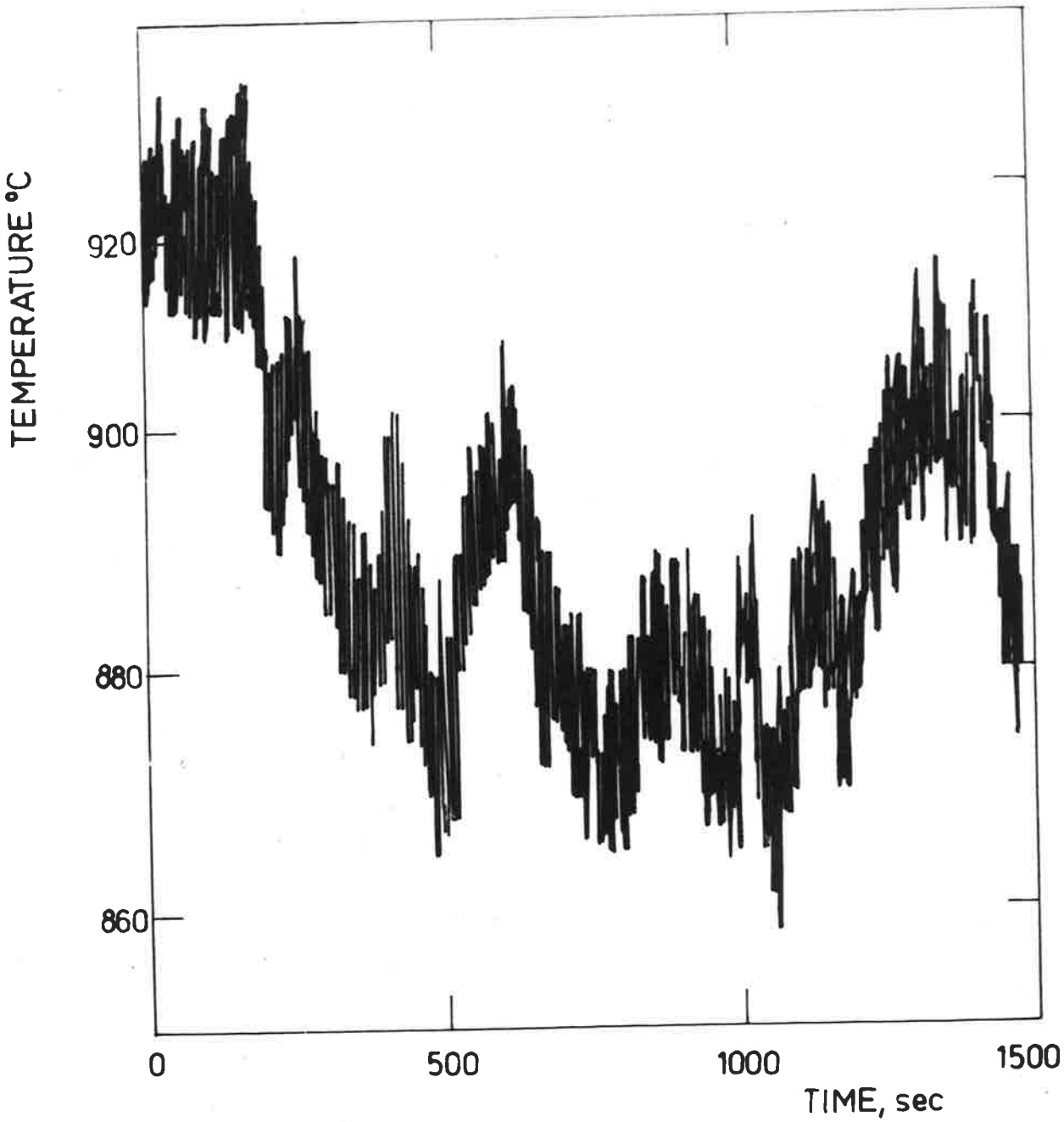

Fig. 7b Output signal of the exp. No. 3

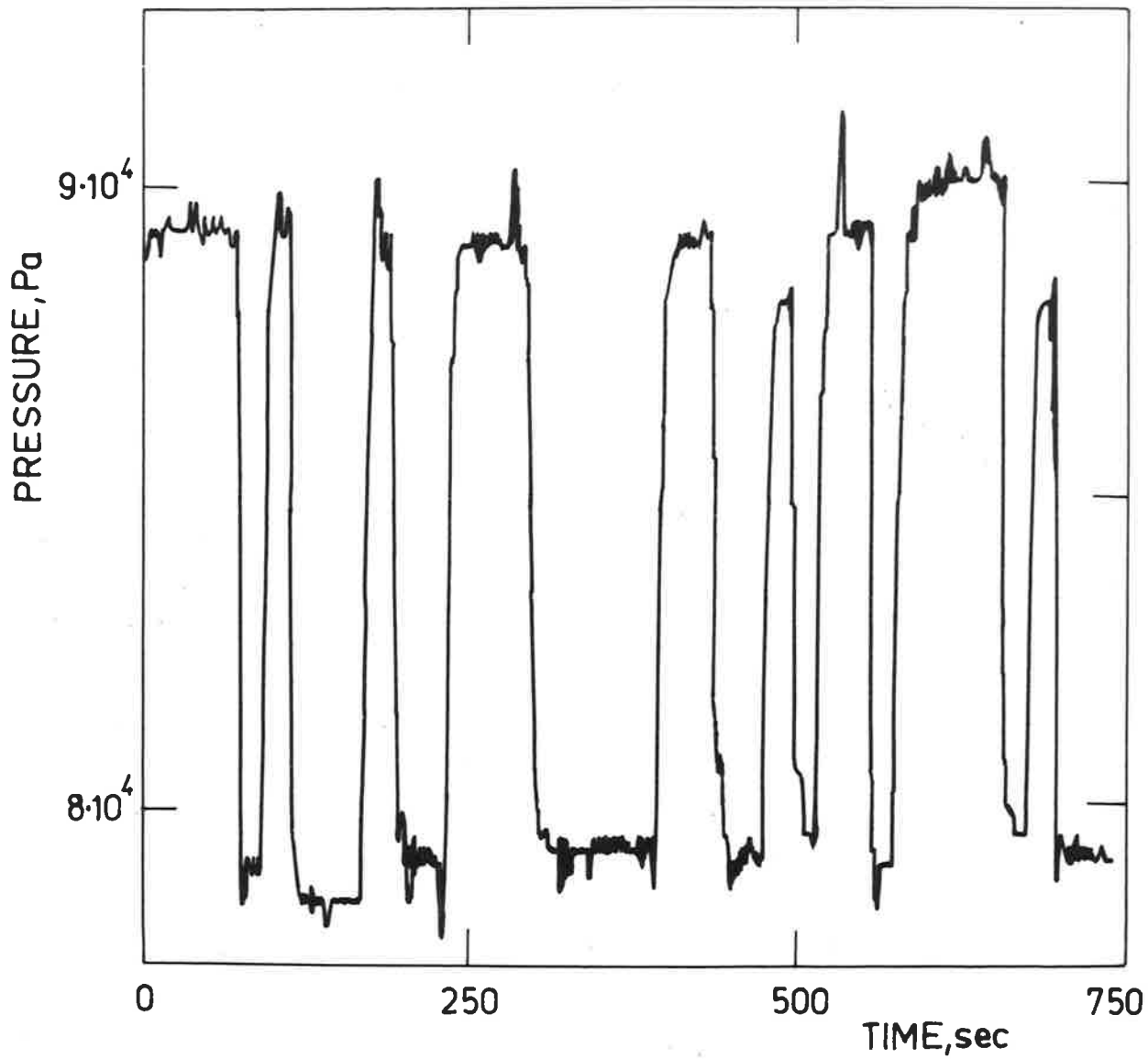

Fig. 8a Input signal of the exp. No. 4

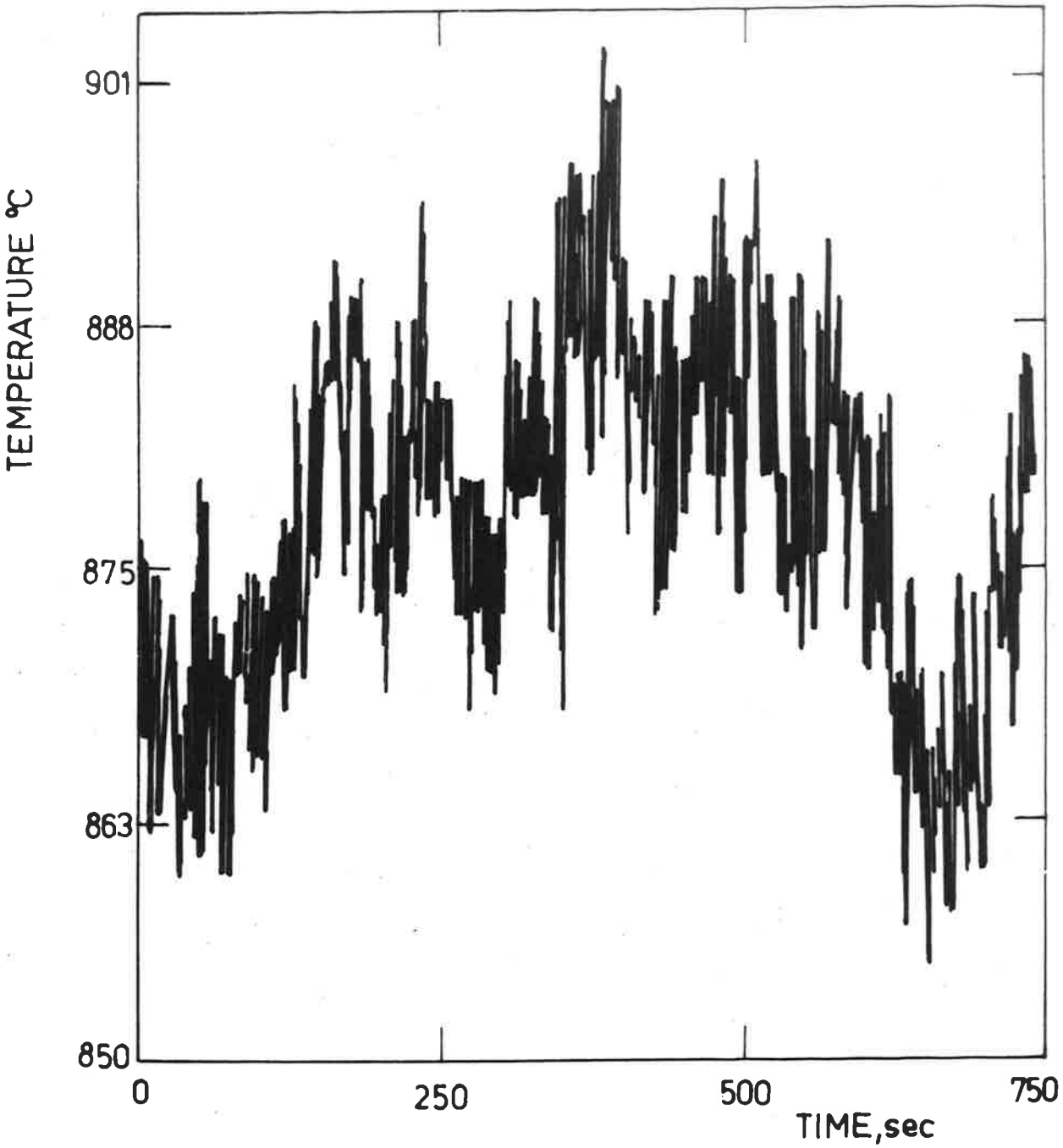

Fig. 8b Output signal of the exp. No. 4

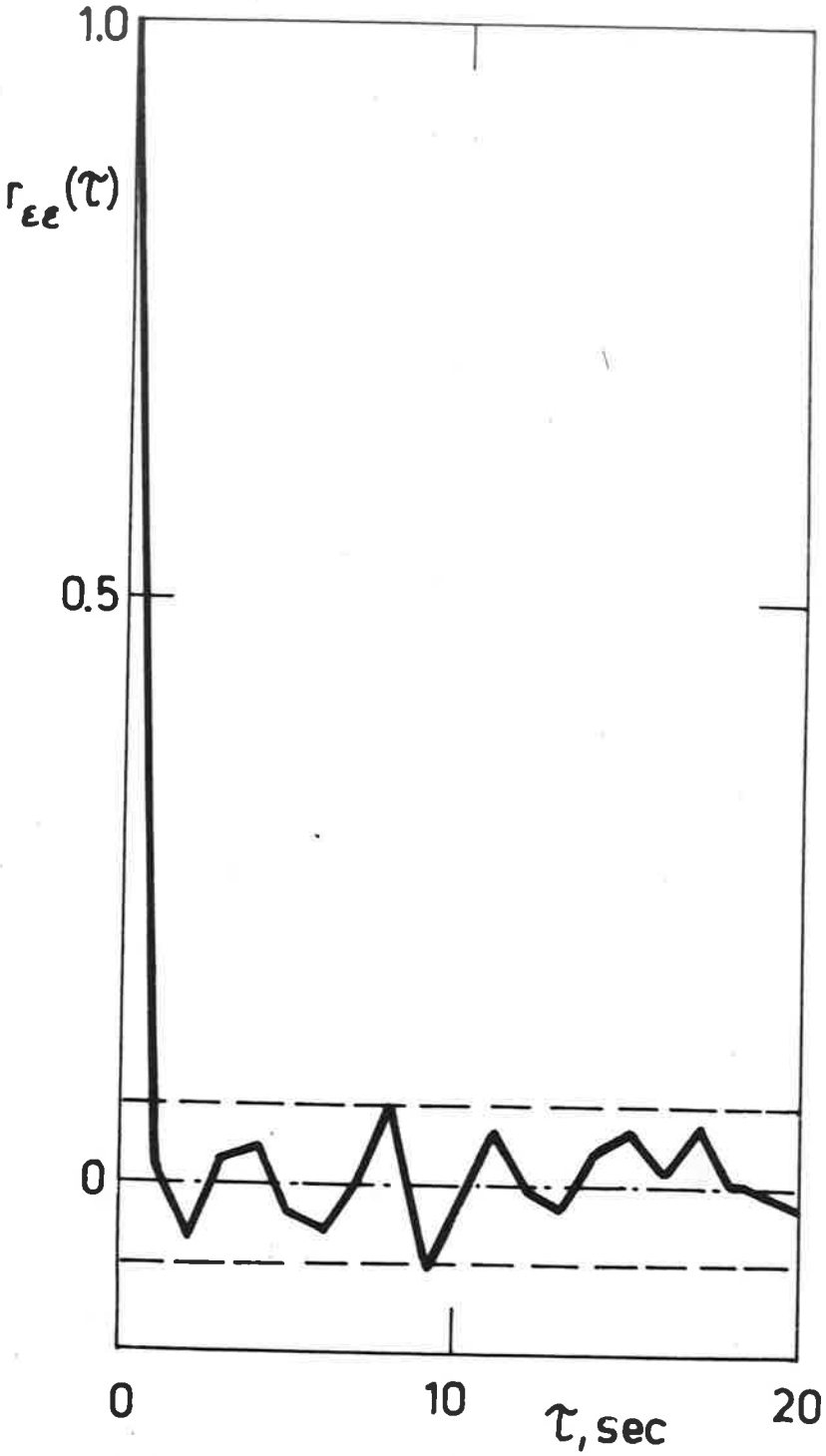

Fig. 9a Normalized autocorrelation function of the residuals for the exp. No. 1

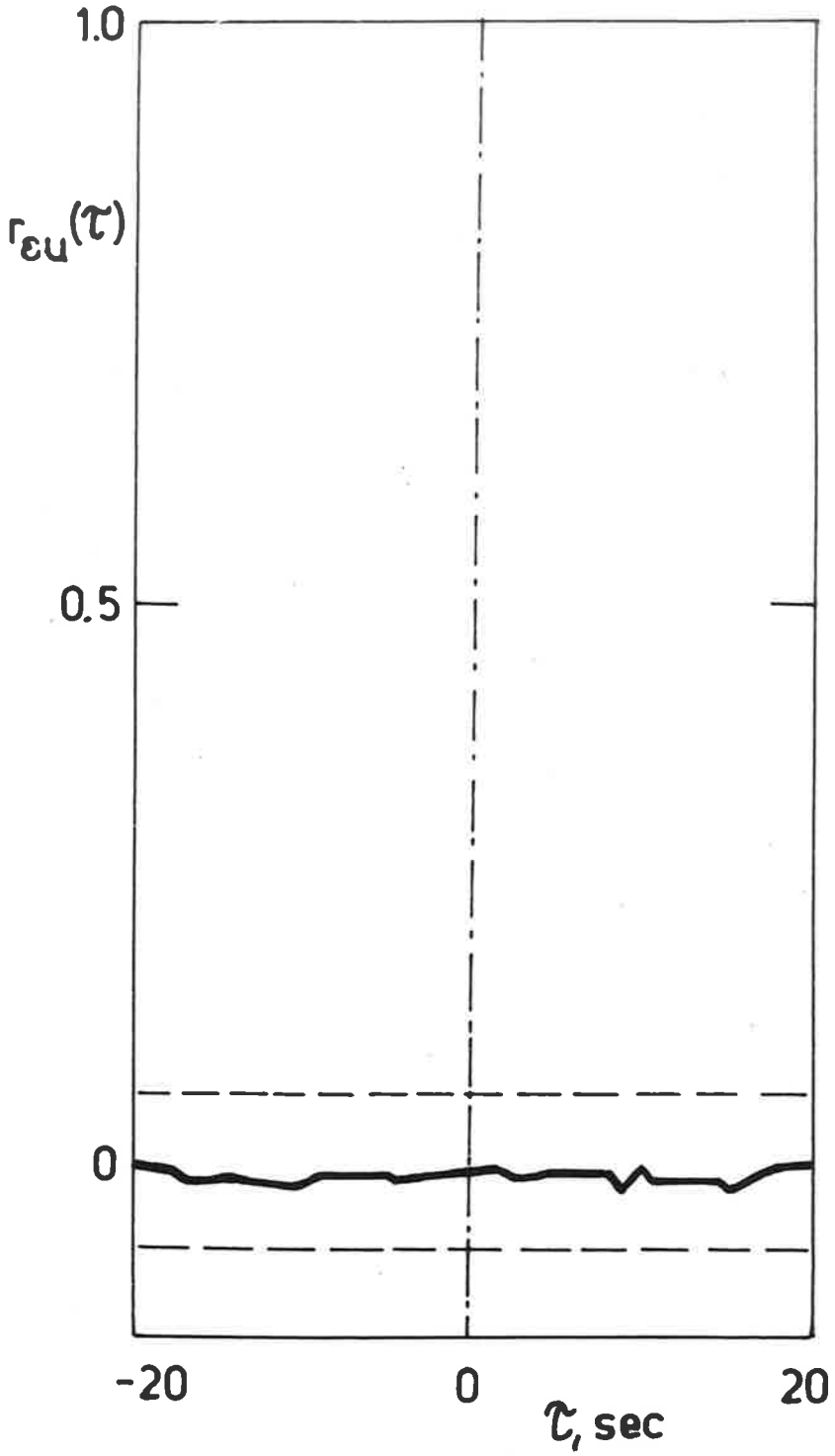

Fig. 9b Crosscorrelation function between residuals and input for the exp. No. 1

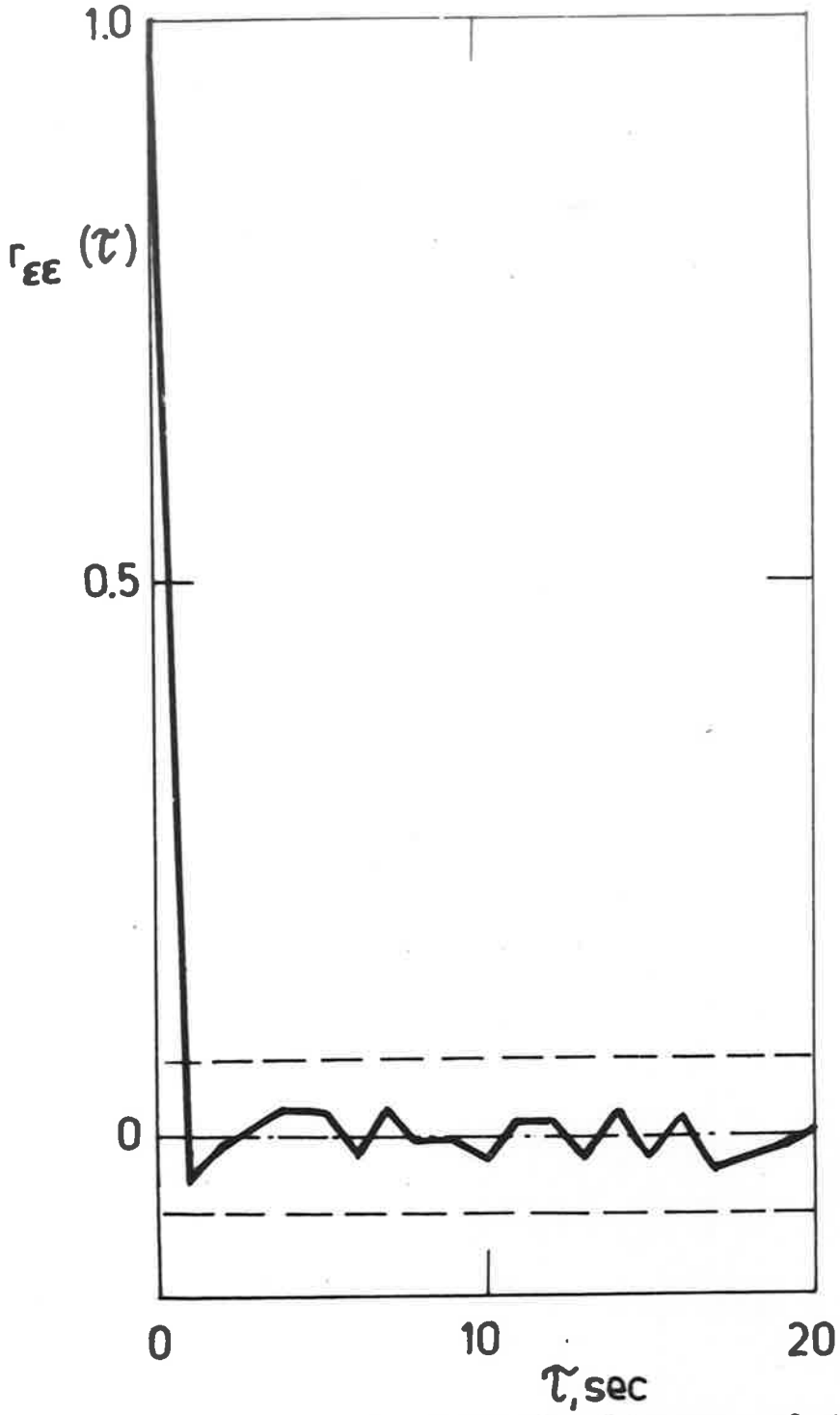

Fig. 10a Normalized autocorrelation function of the residuals for the exp. No. 2

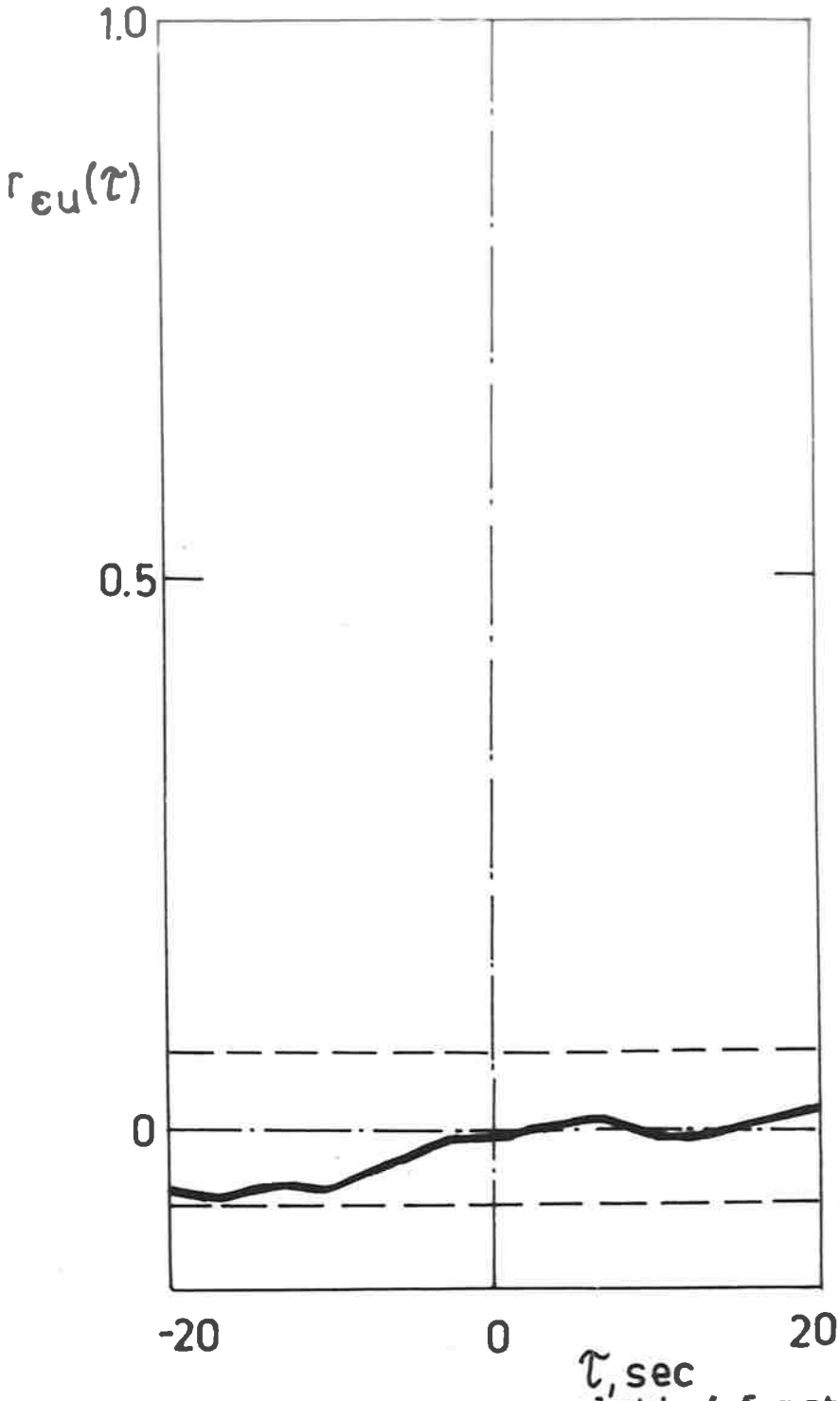

Fig. 10b Crosscorrelation function between residuals and input for the exp. No. 2

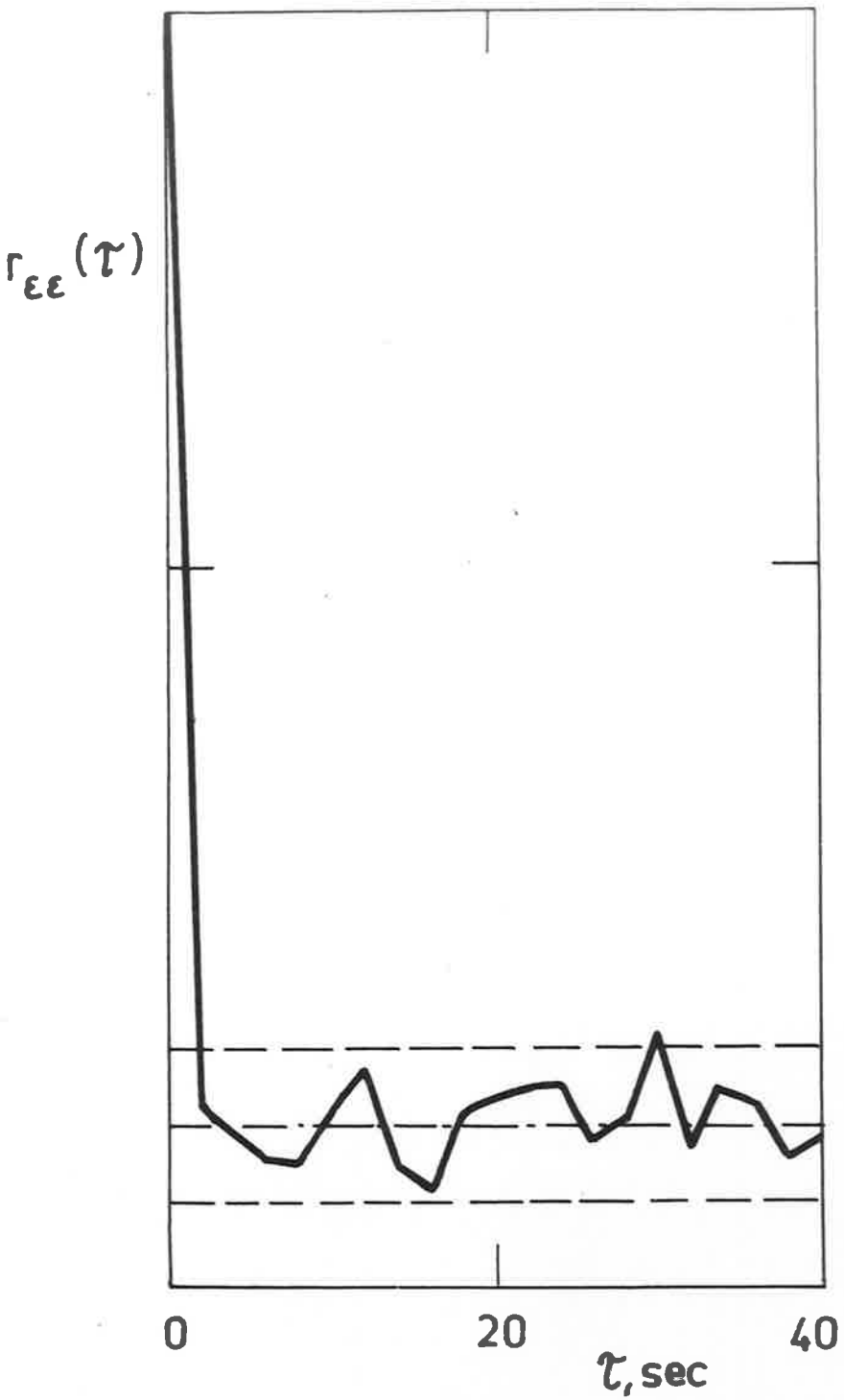

Fig. 11a Normalized autocorrelation function of the residuals for the exp. No. 2

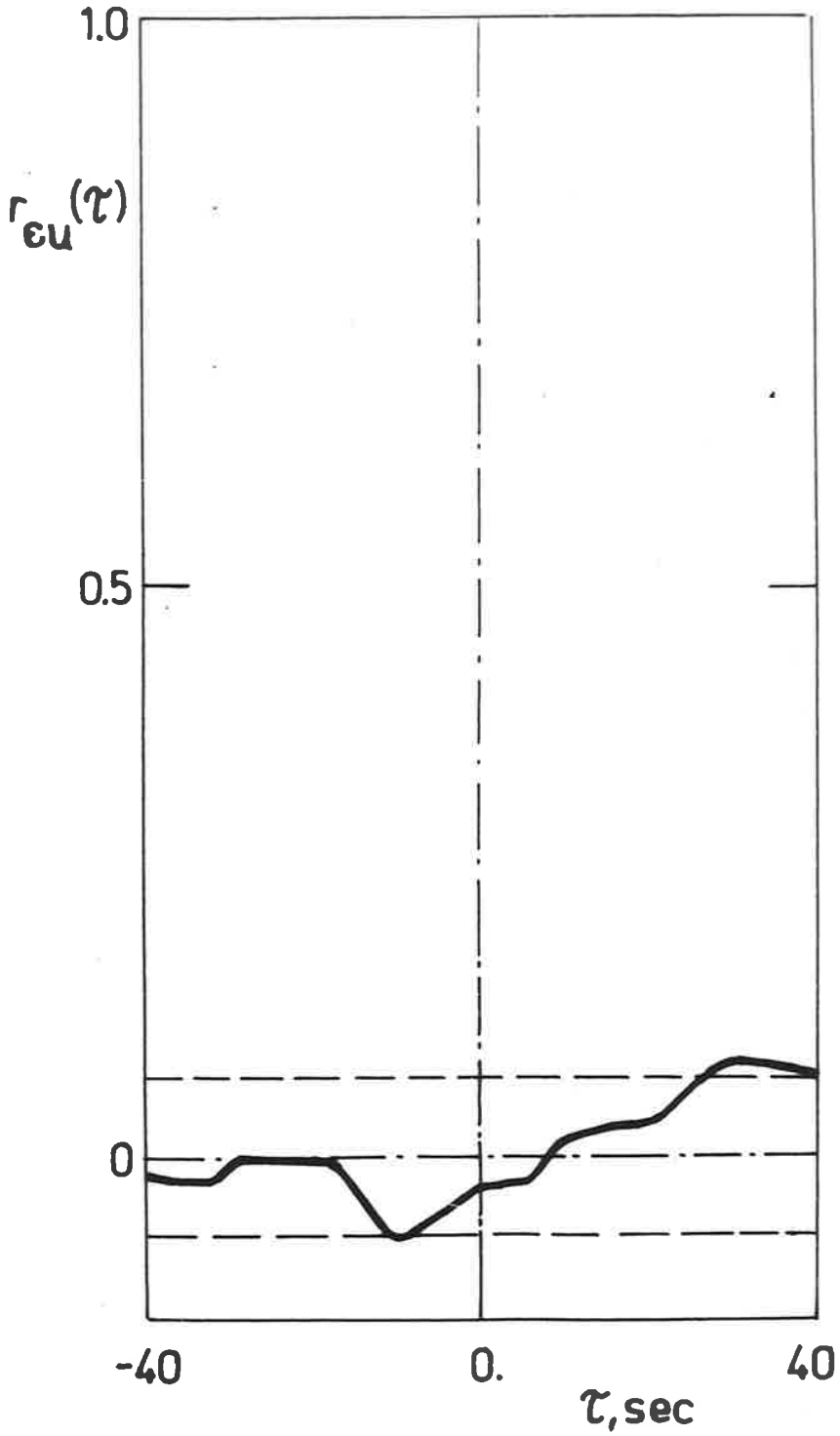

Fig. 11b Crosscorrelation function between residuals and input for the exp. No. 3

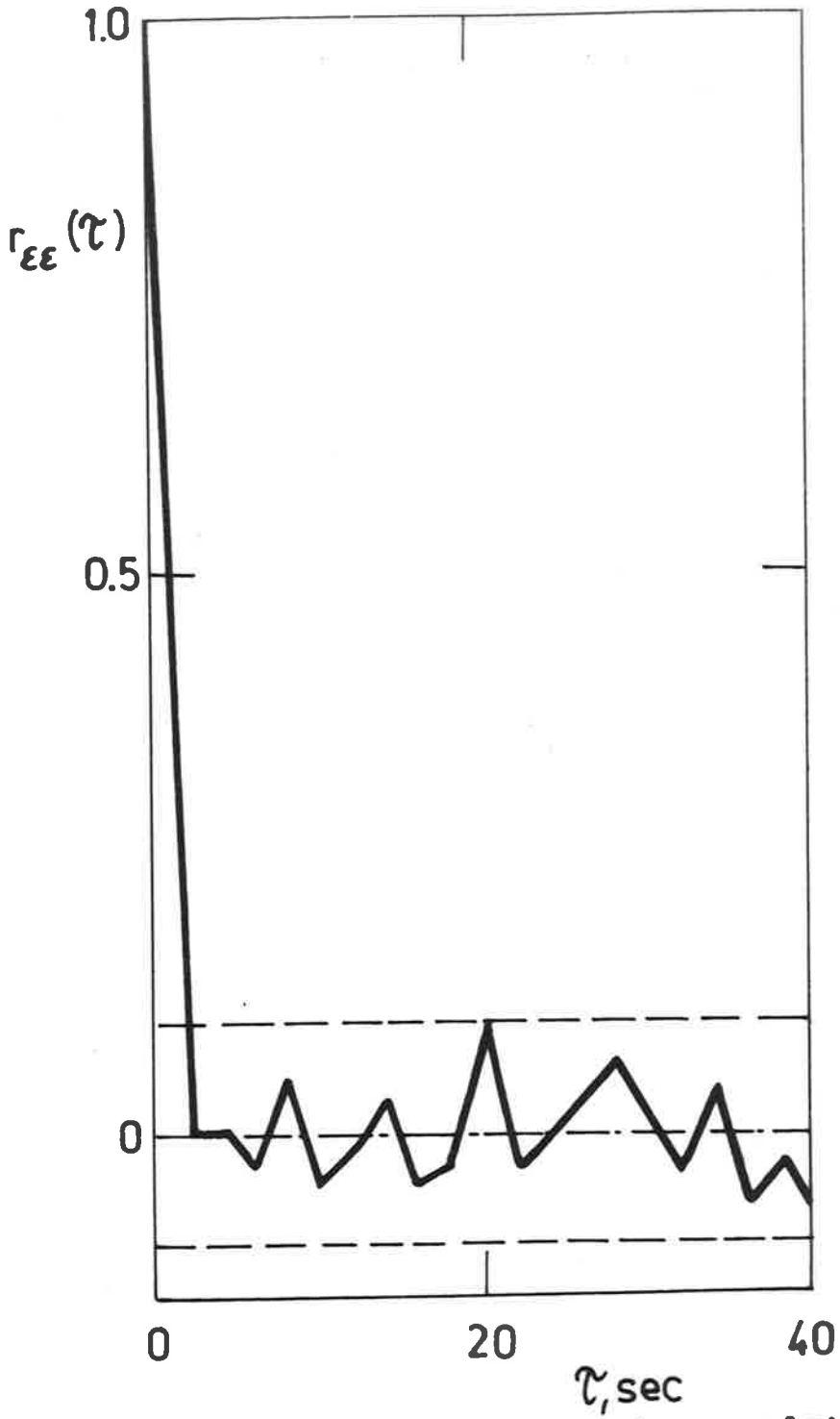

Fig. 12a Normalized autocorrelation function of the residuals for the exp. No. 4

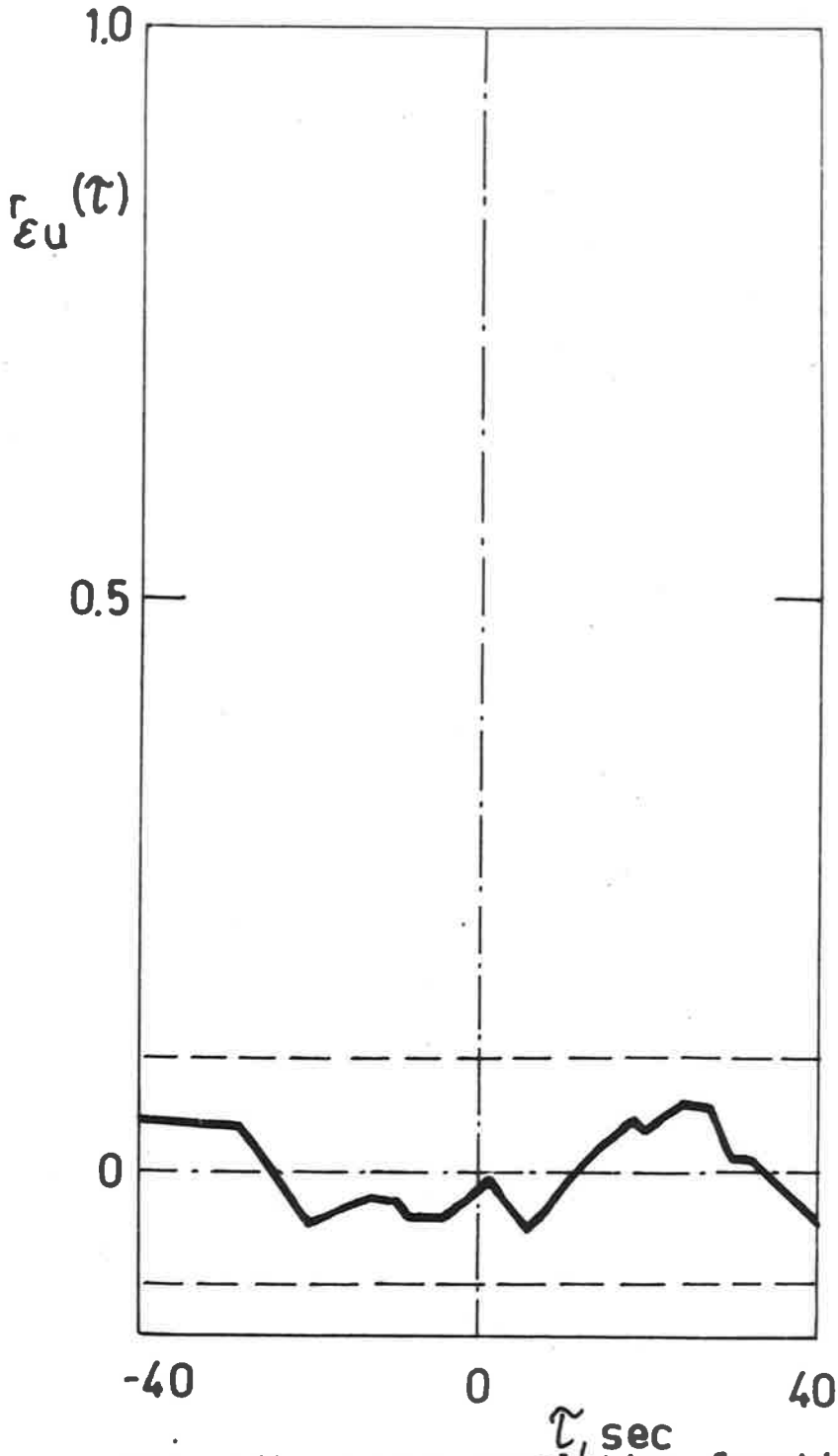

Fig. 12b Crosscorrelation function between residuals and input for the exp. No. 4

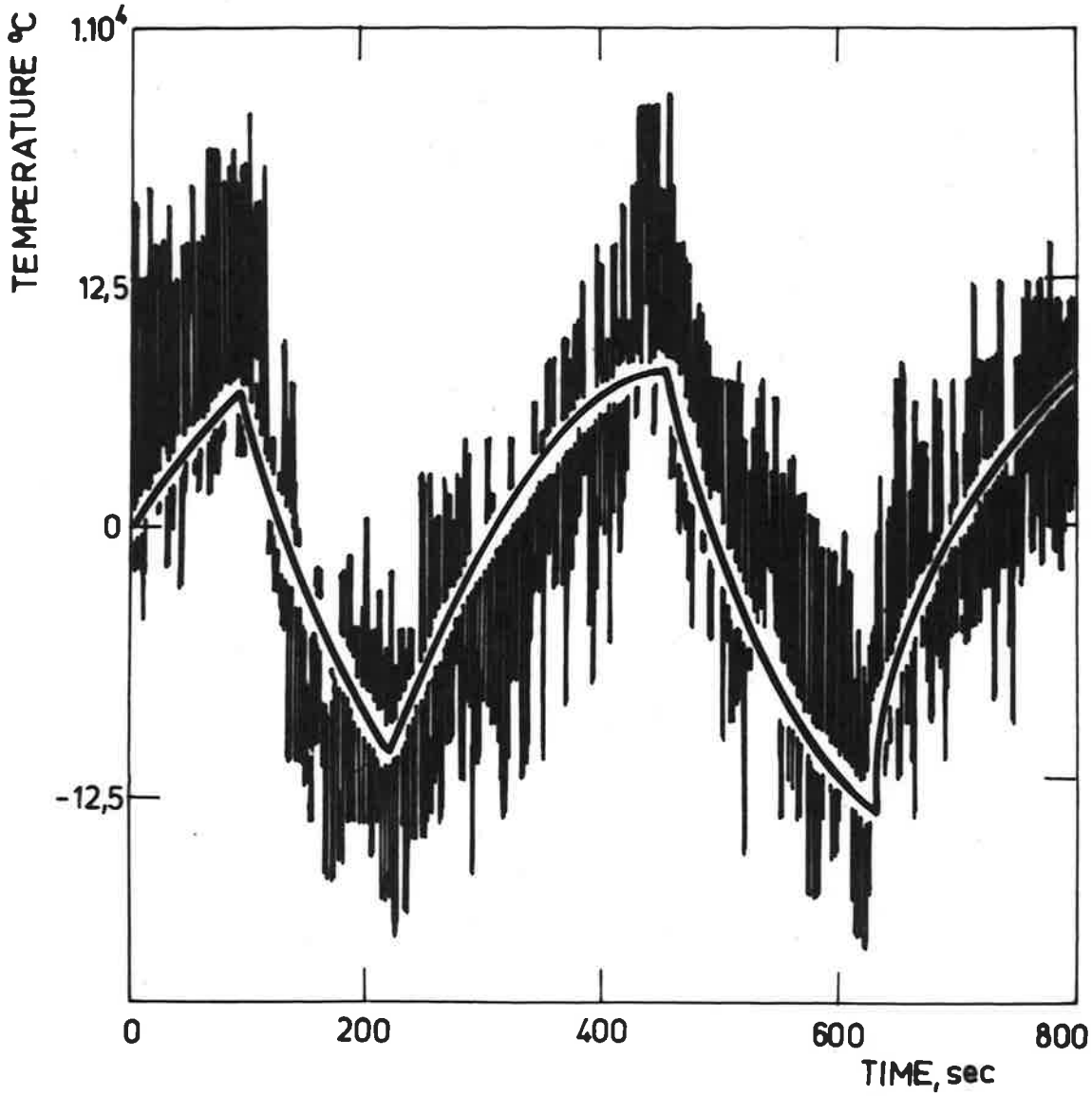

Fig. 13 Comparison between the measured output (with higher frequences) and the deterministic model output for the exp. No. 1

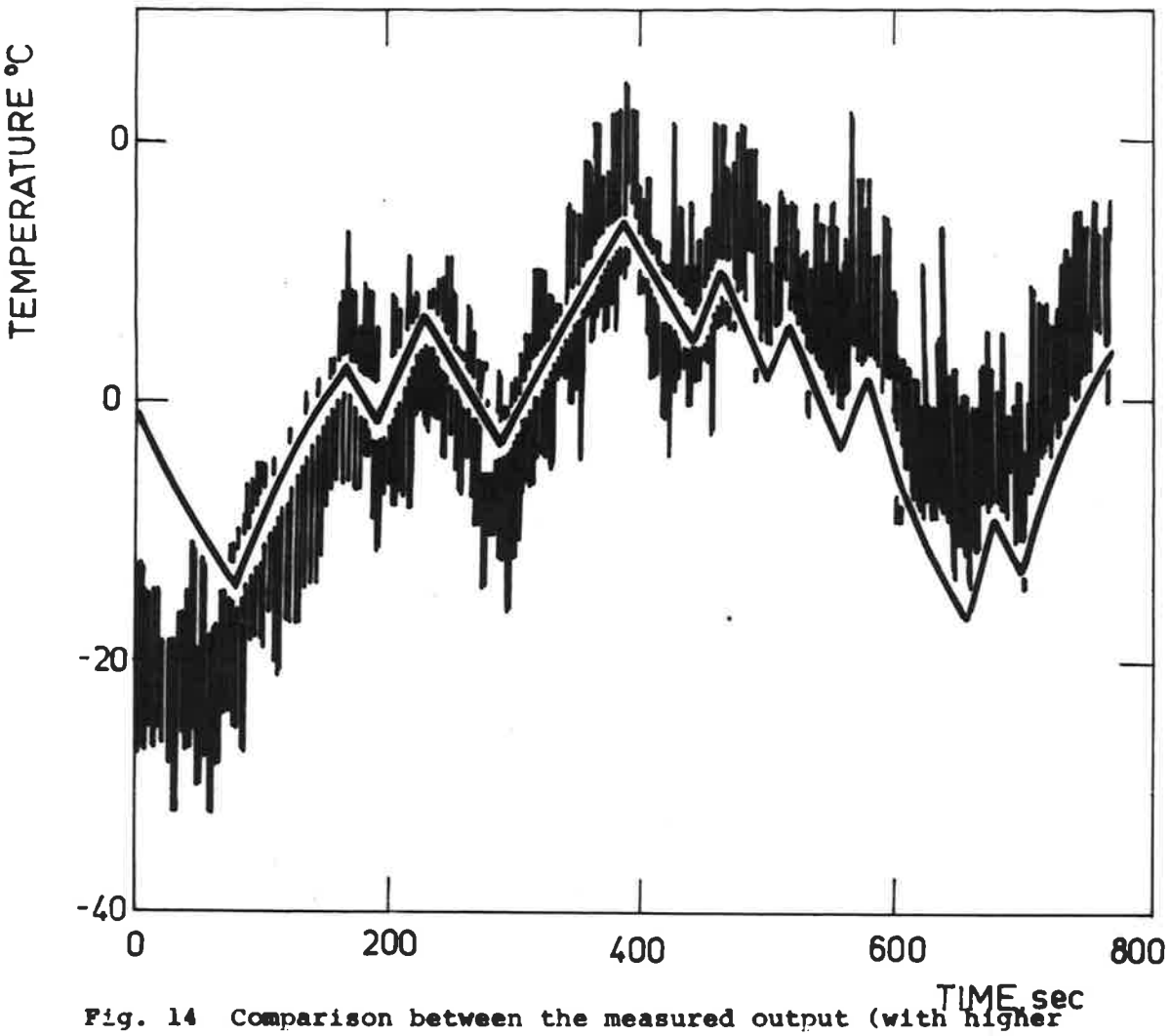

Fig. 14 Comparison between the measured output (with higher frequences) and the deterministic model output for the exp. No. 2

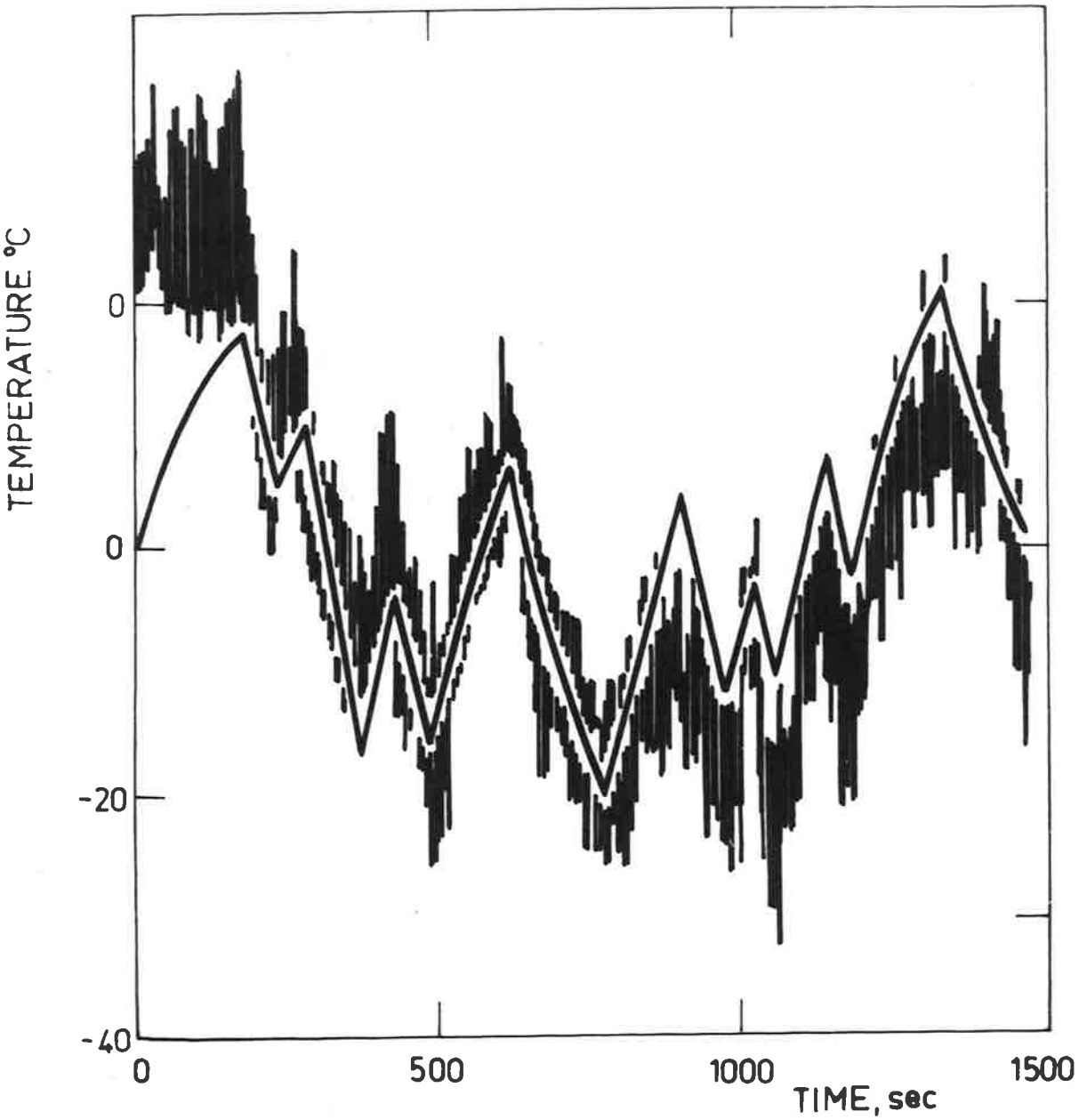

Fig. 15 Comparison between the measured output (with higher frequences) and the deterministic model output for the exp. No. 3

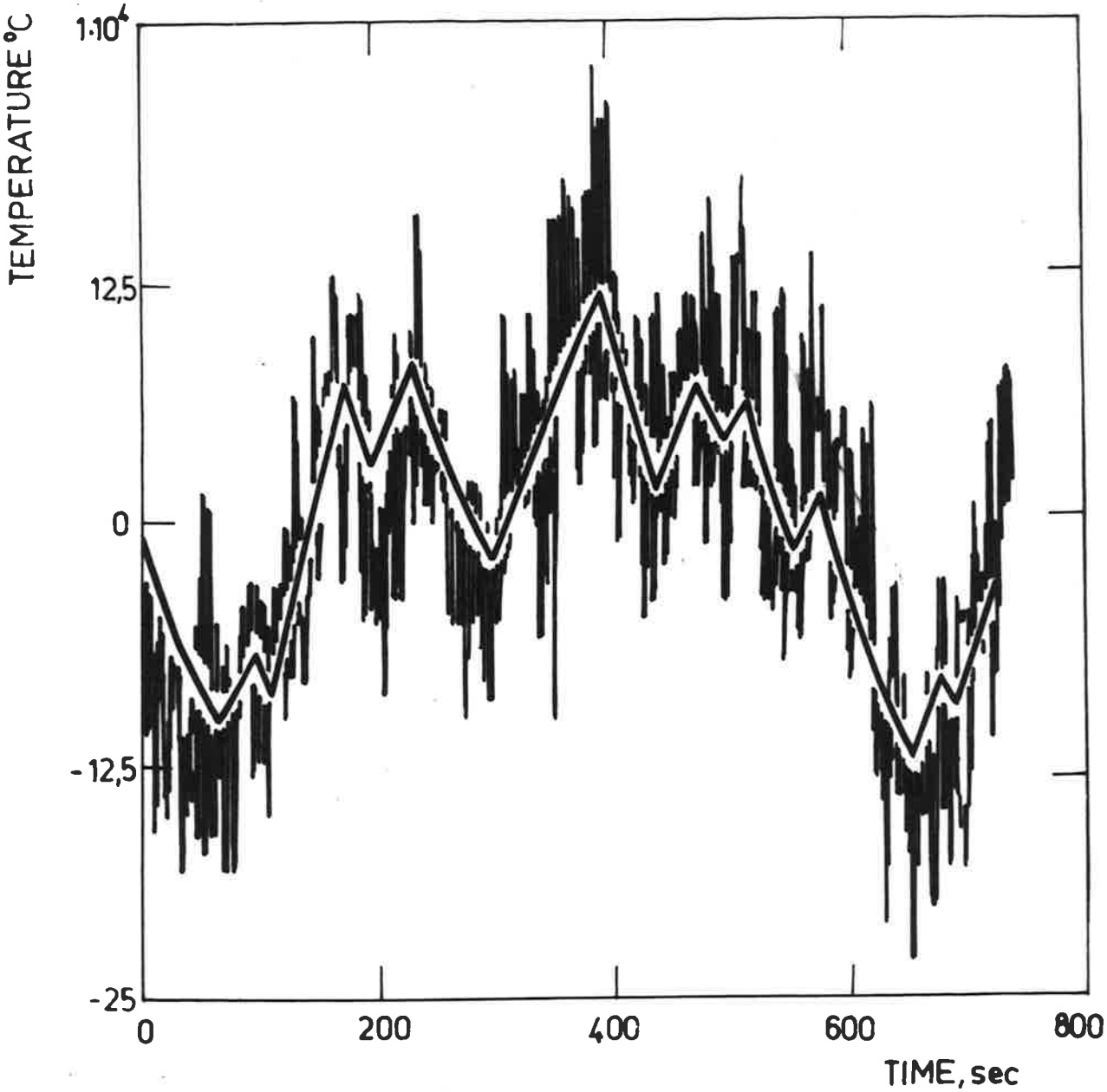

Fig. 16 Comparison between the measured output (with higher frequences) and the deterministic model output for the exp. No. 4

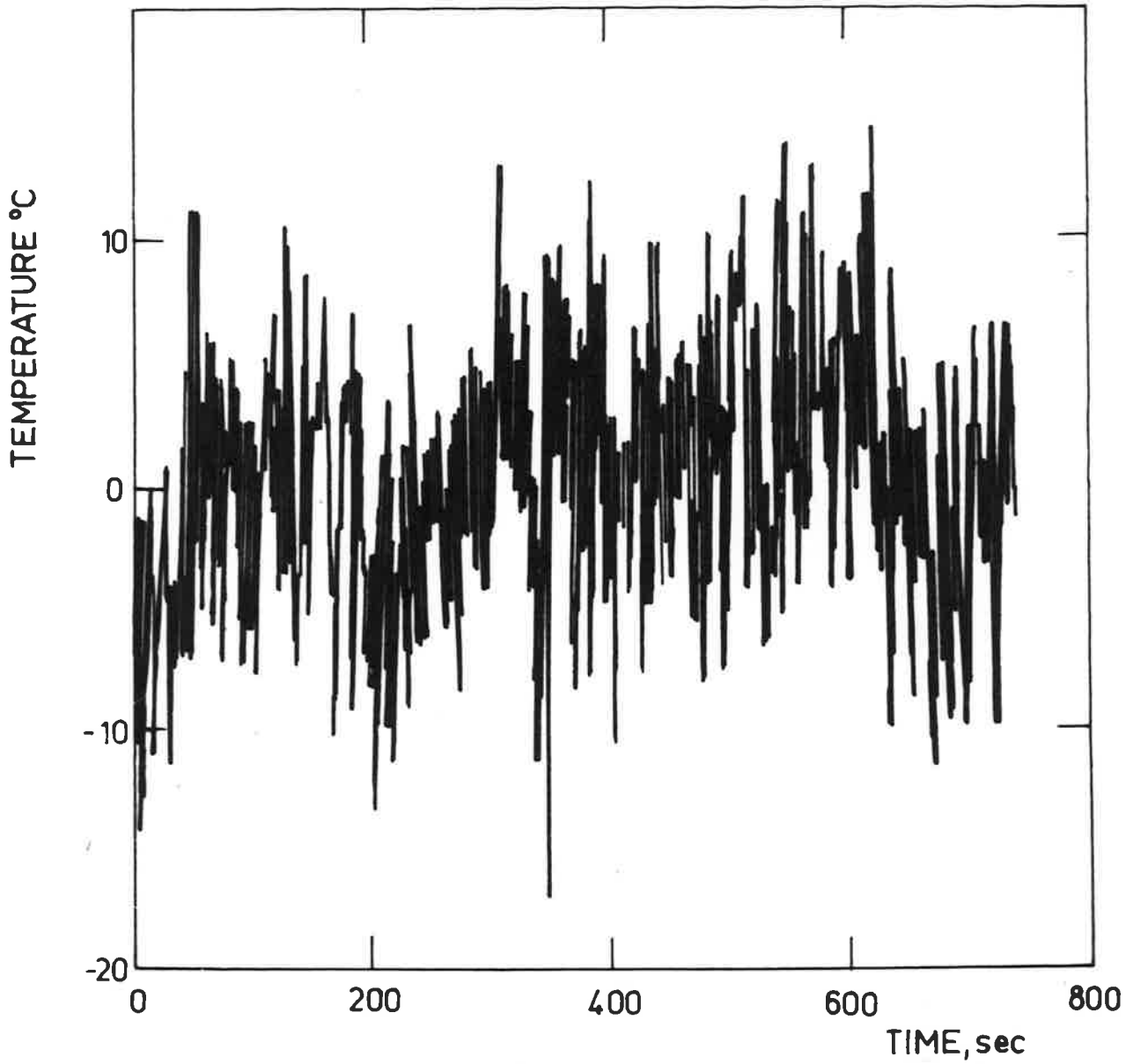

Fig. 17 Plot of the residuals for the first order model for the exp. No. 4

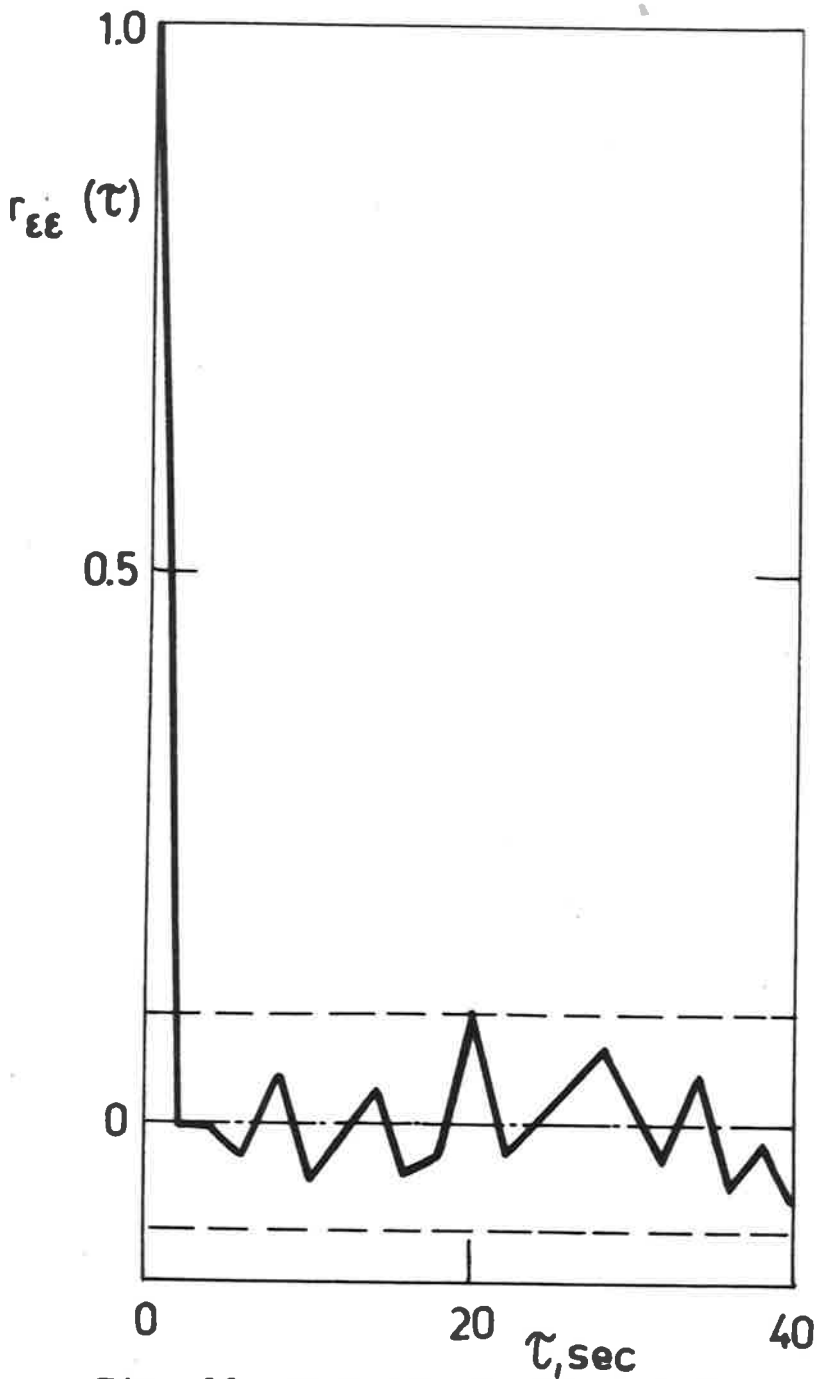

Fig. 18 Normalized autocorrelation function of the residuals of the exp. No. 4

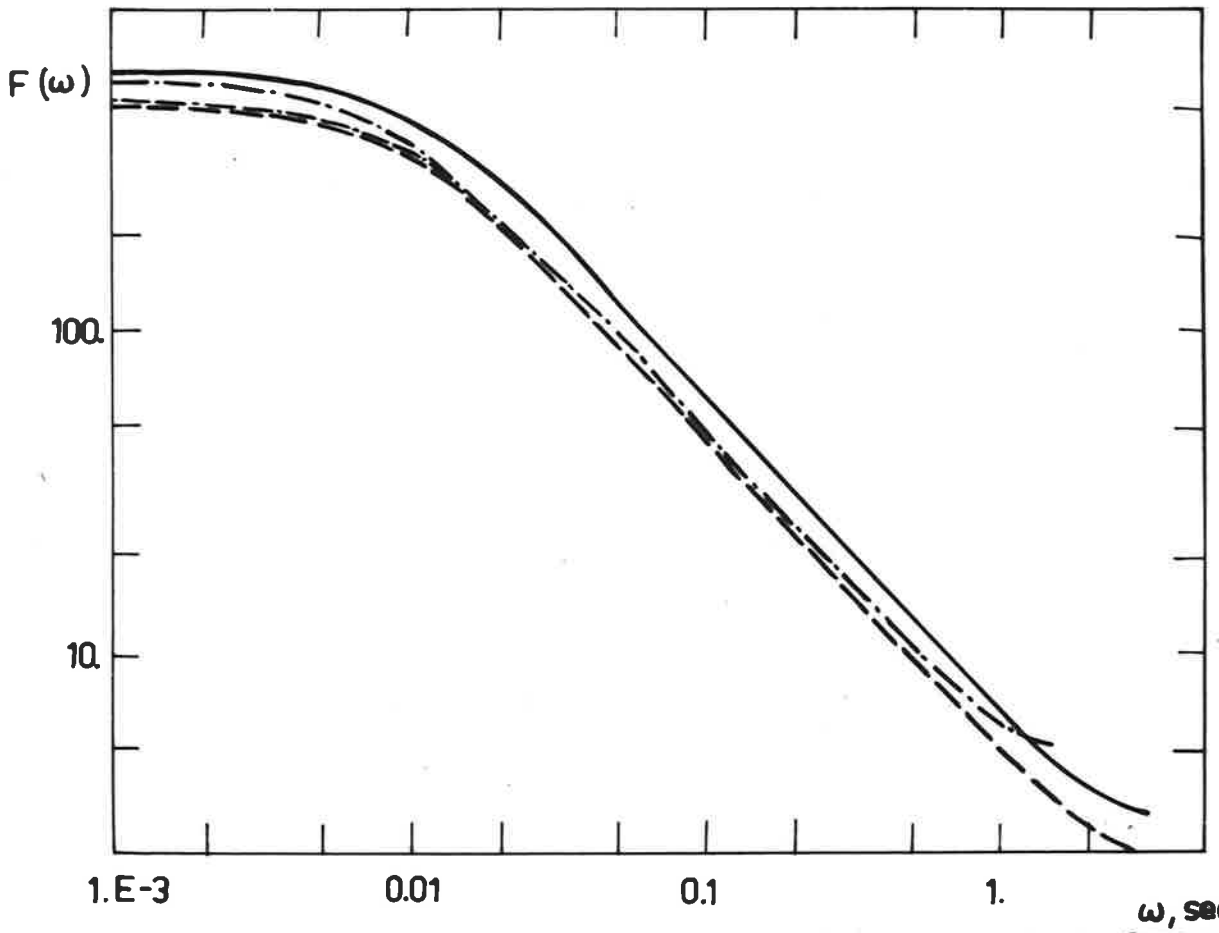

Fig. 19 Comparison between the gains of the frequency response functions for the exp. No. 1-4. Exp. No. 1 ——— , No. 2 _ _ _ _ , No. 3 _ . _ . _ . _ , No. 4 _ _ . _ _ .

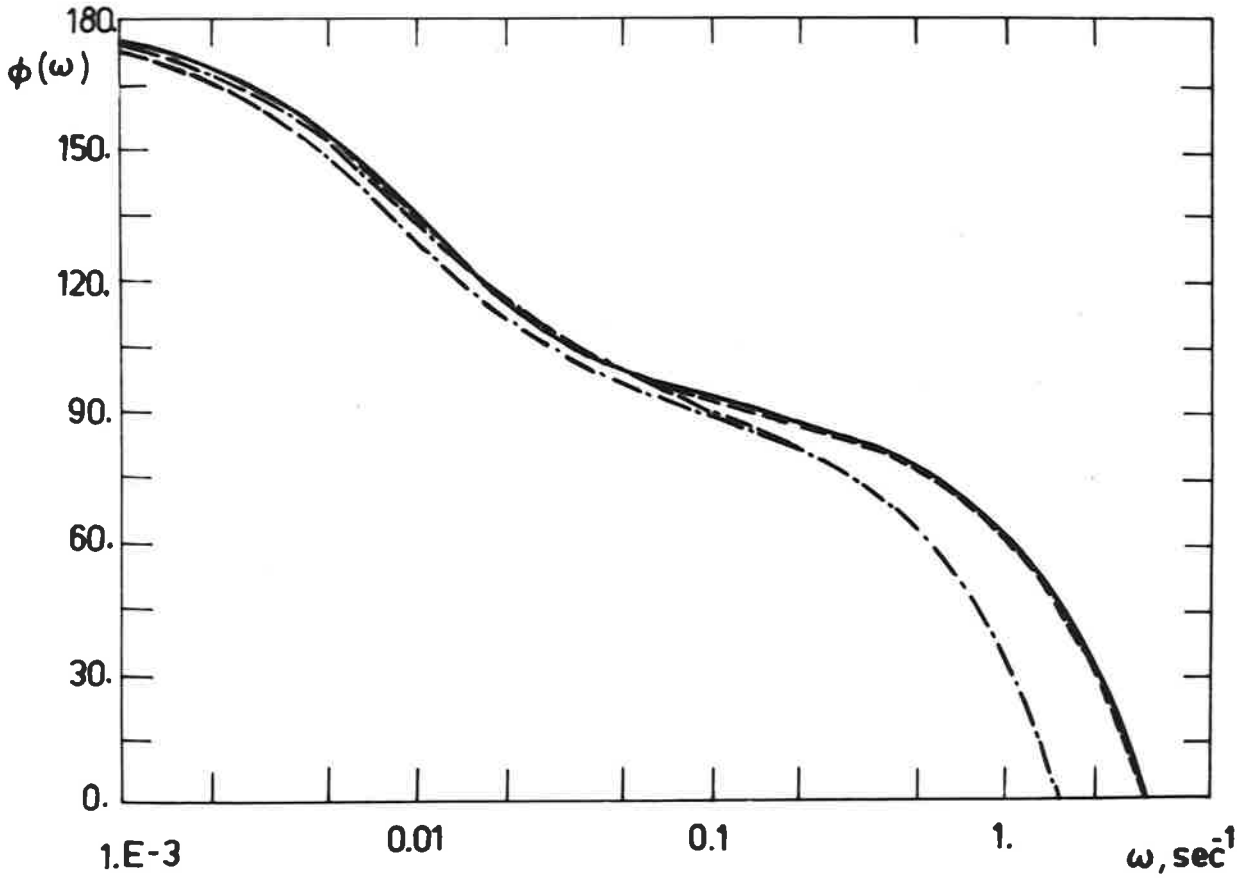

Fig. 20 Comparison between the phase of the frequency response functions for the exp. No. 1-4. Exp. No. 1 _____, No. 2 _ _ _ _ , No. 3 _ - _ . _ . _ , No. 4. _ _ . _ _ .

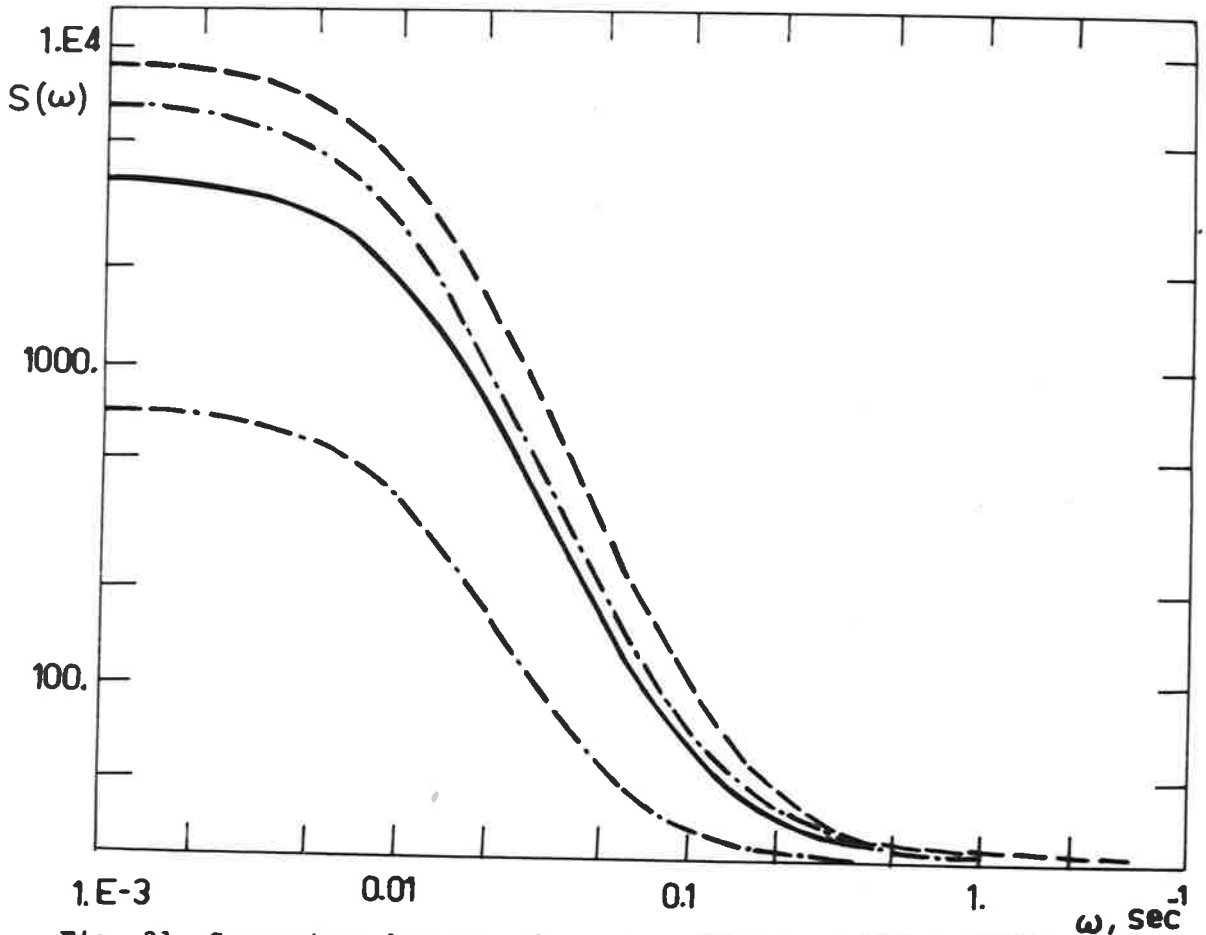

Fig. 21 Comparison between the power spectra of the disturbances for the exp. No. 1-4. Exp. No. 1 _____ , No. 2 _ _ _ _ , No. 3 _ . _ . _ , No. 4 _ _ , _ _ .

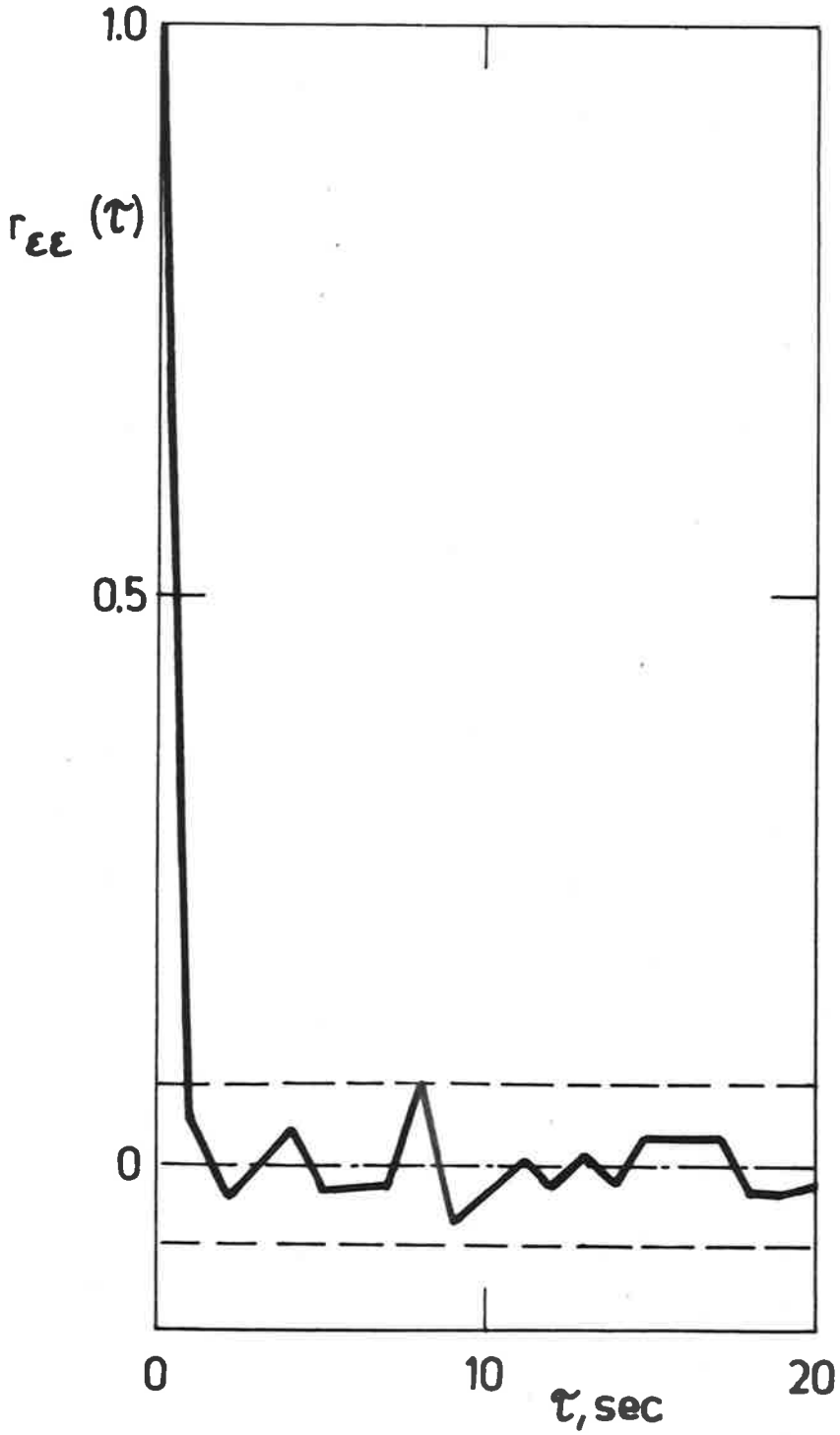

Fig. 22a Normalized autocorrelation function of the residuals for the exp. No. 1

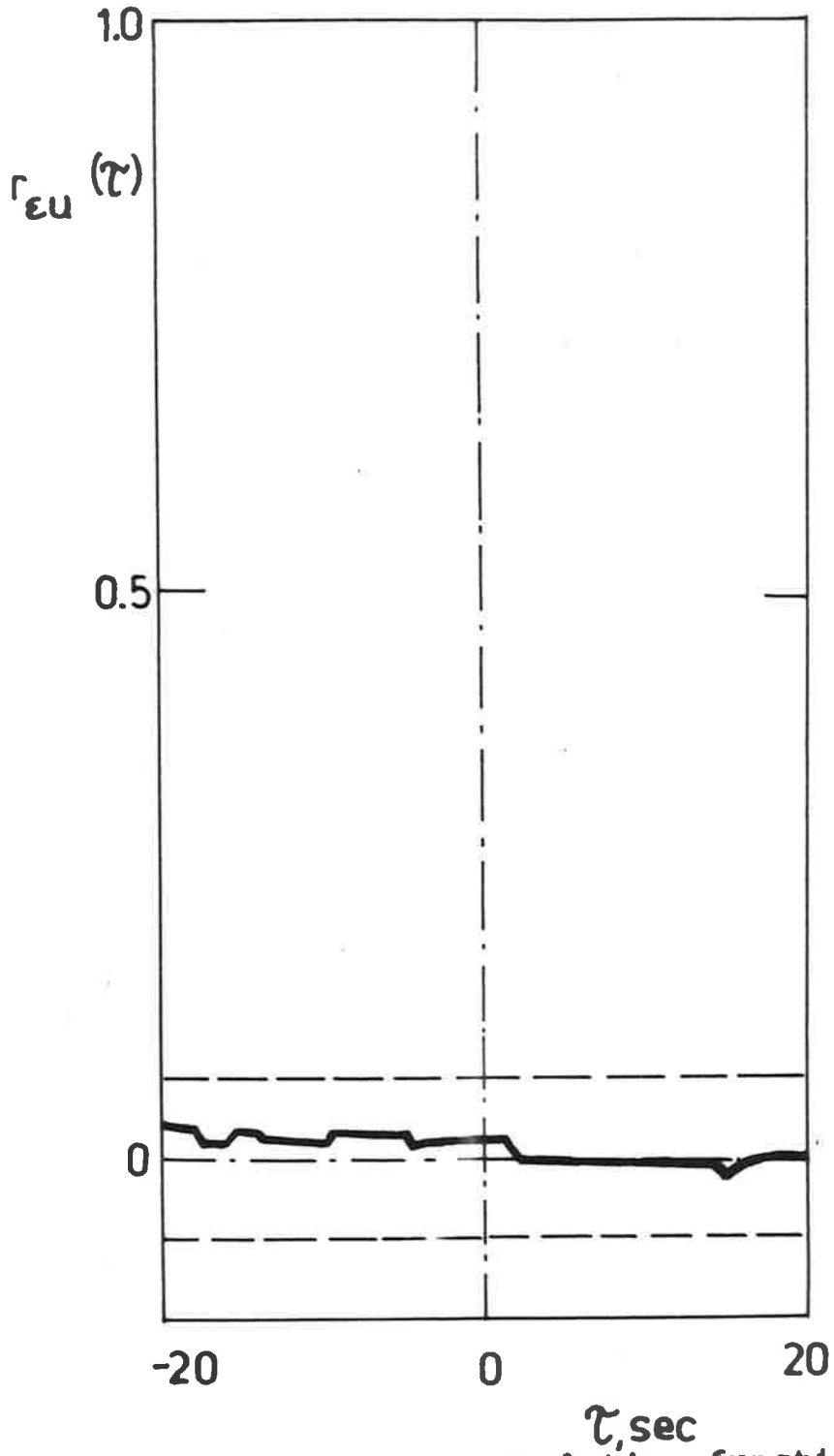

Fig. 22b Crosscorrelation function between residuals and input for the exp. No. 1

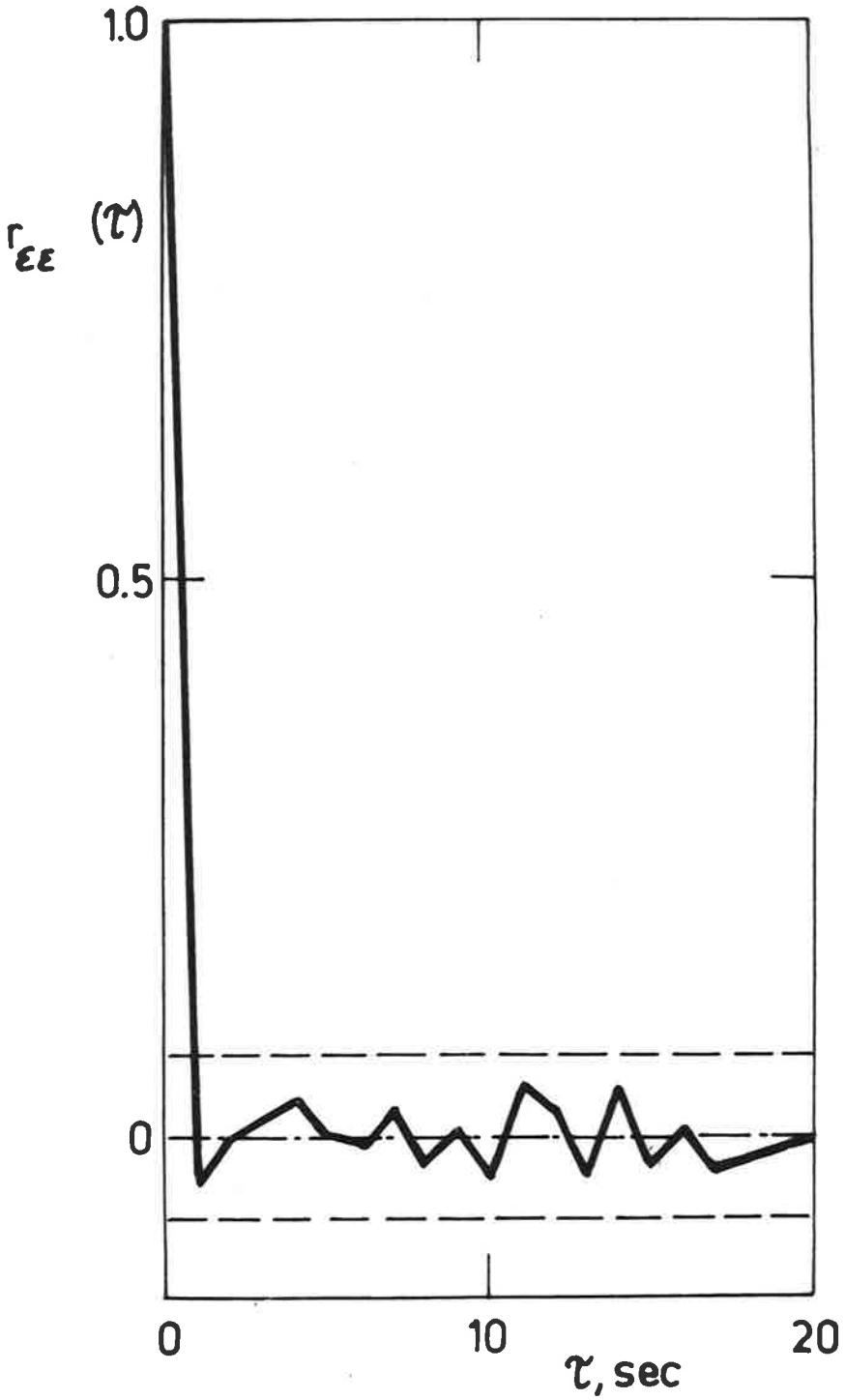

Fig. 23a Normalized autocorrelation function of the residuals for the exp. No. 2

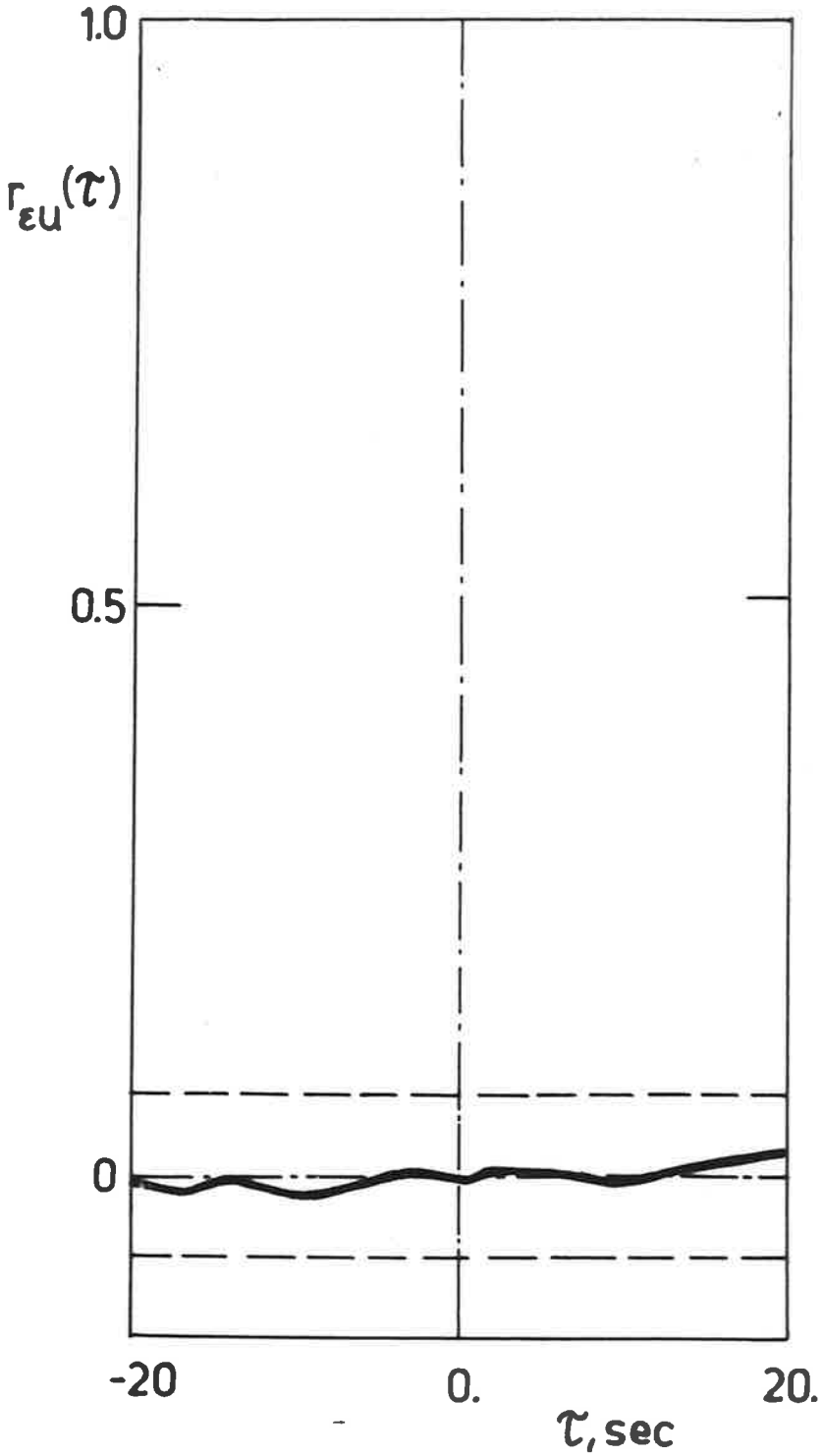

Fig. 23b Crosscorrelation function between residuals and input for the exp. No. 2

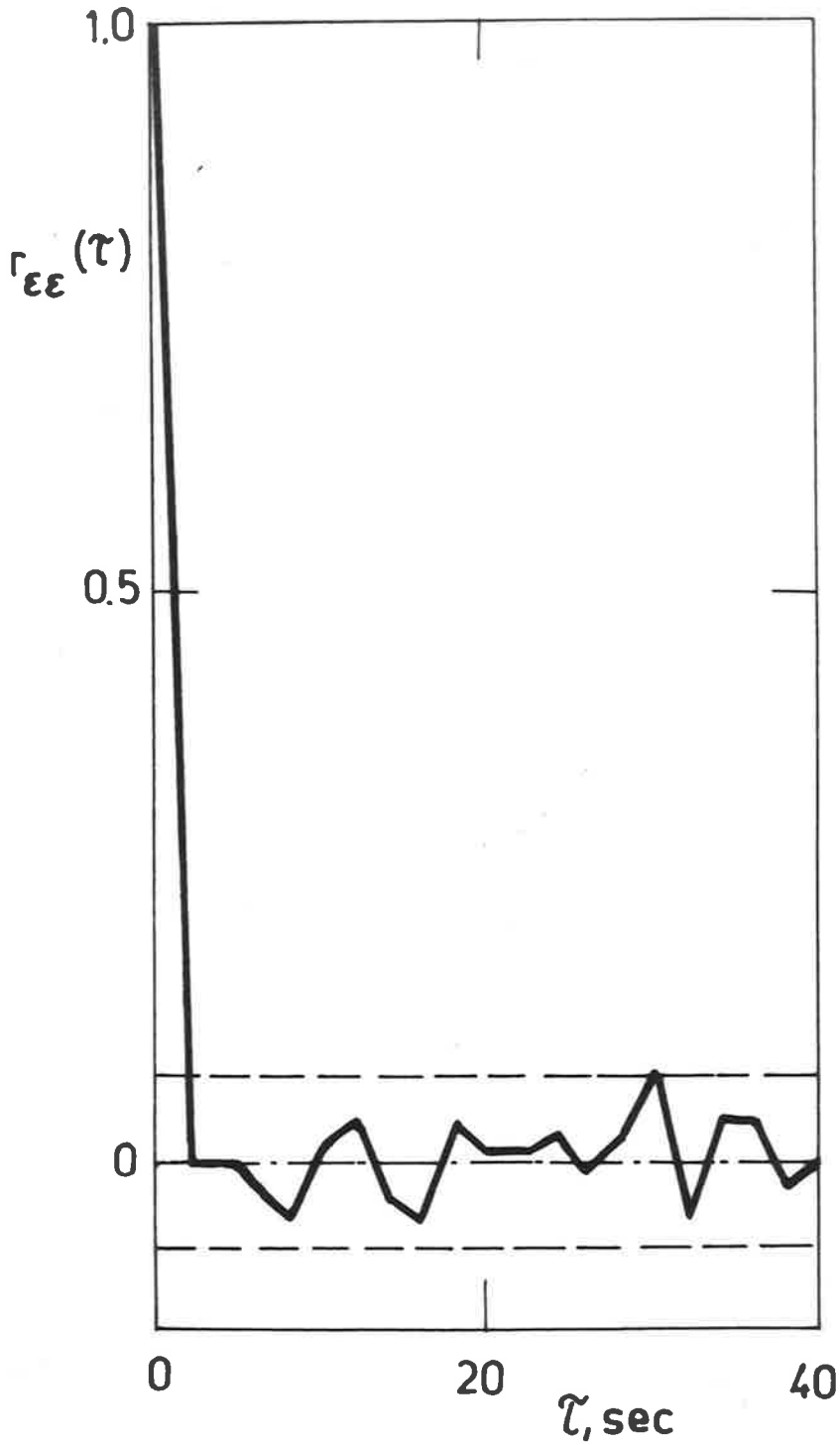

Fig.24a Normalized autocorrelation function of the residuals for the exp. No. 3

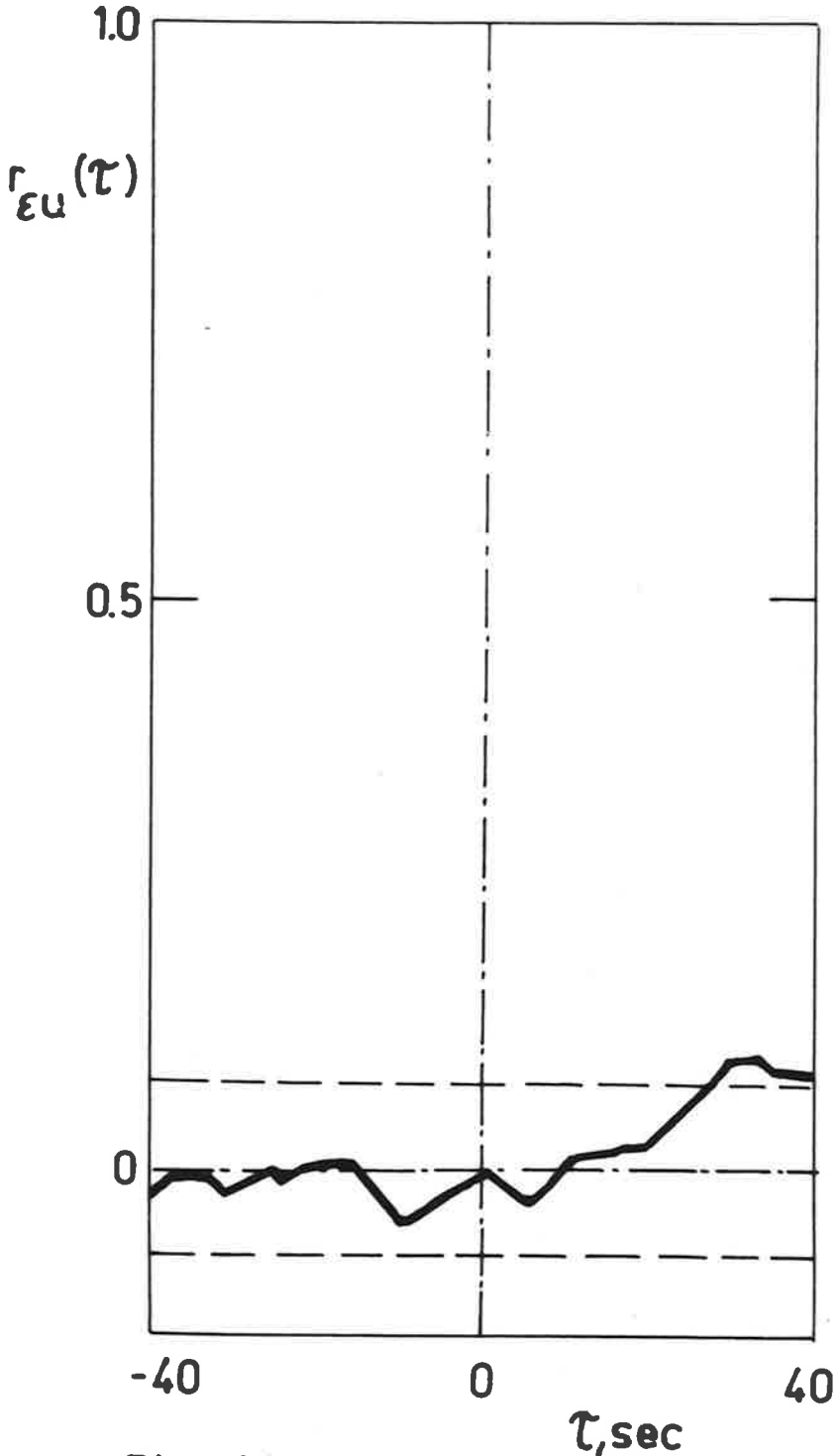

Fig. 24b Crosscorrelation function between residuals and input for the exp. No. 3

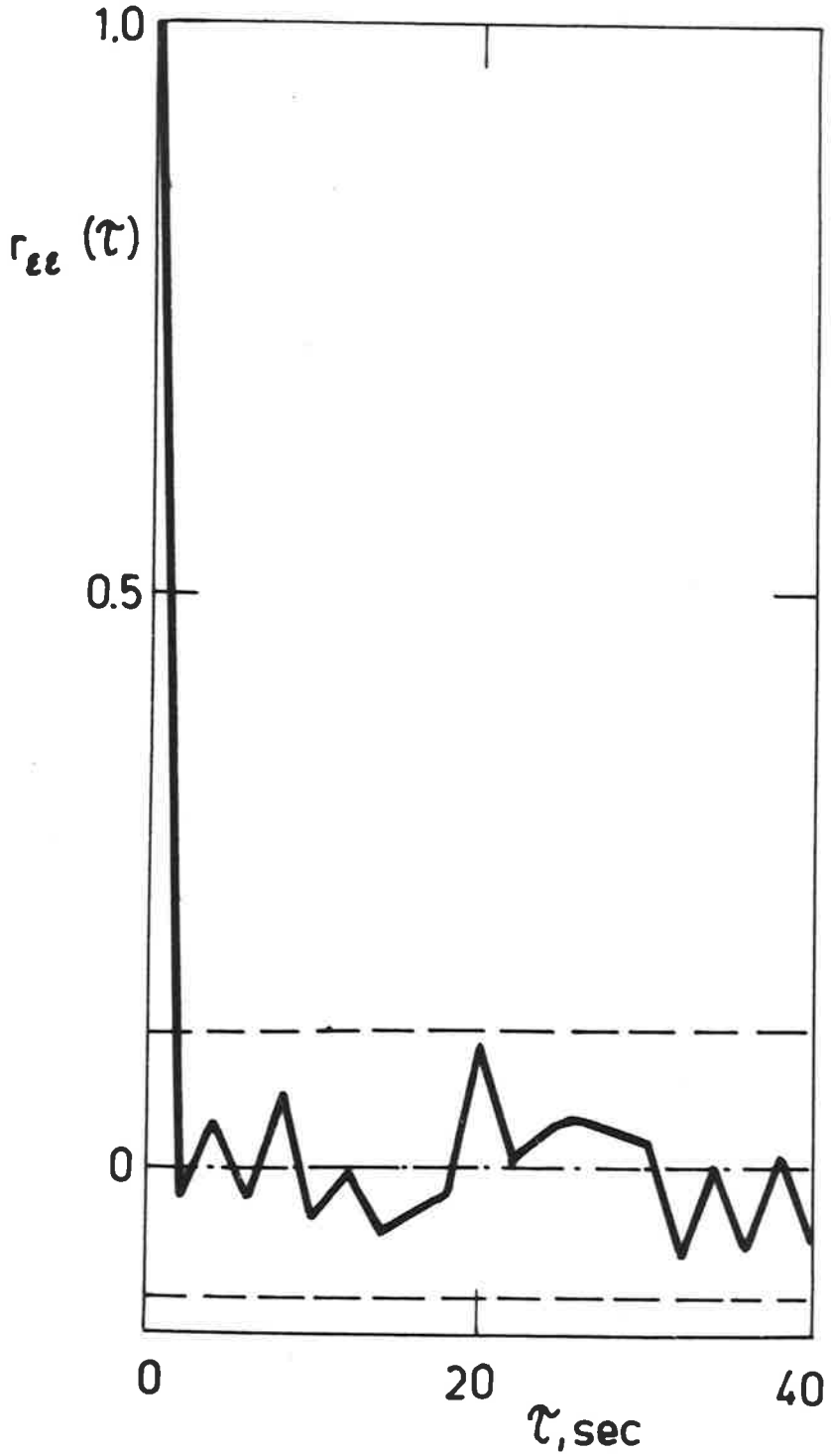

Fig. 25a Normalized autocorrelation function of the residuals for the exp. No. 4

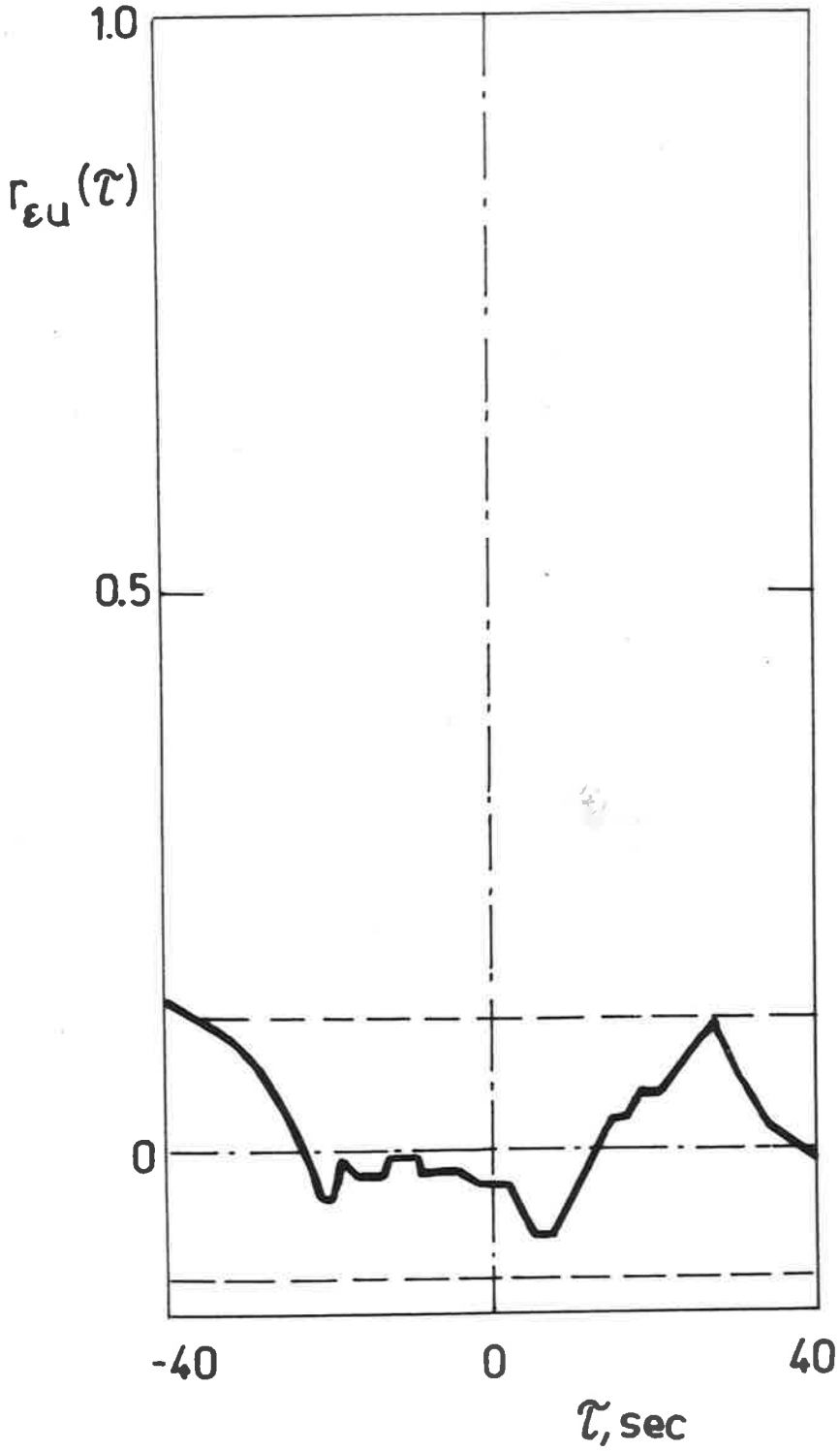

Fig. 25b Crosscorrelation function between residuals and input for the exp. No. 4

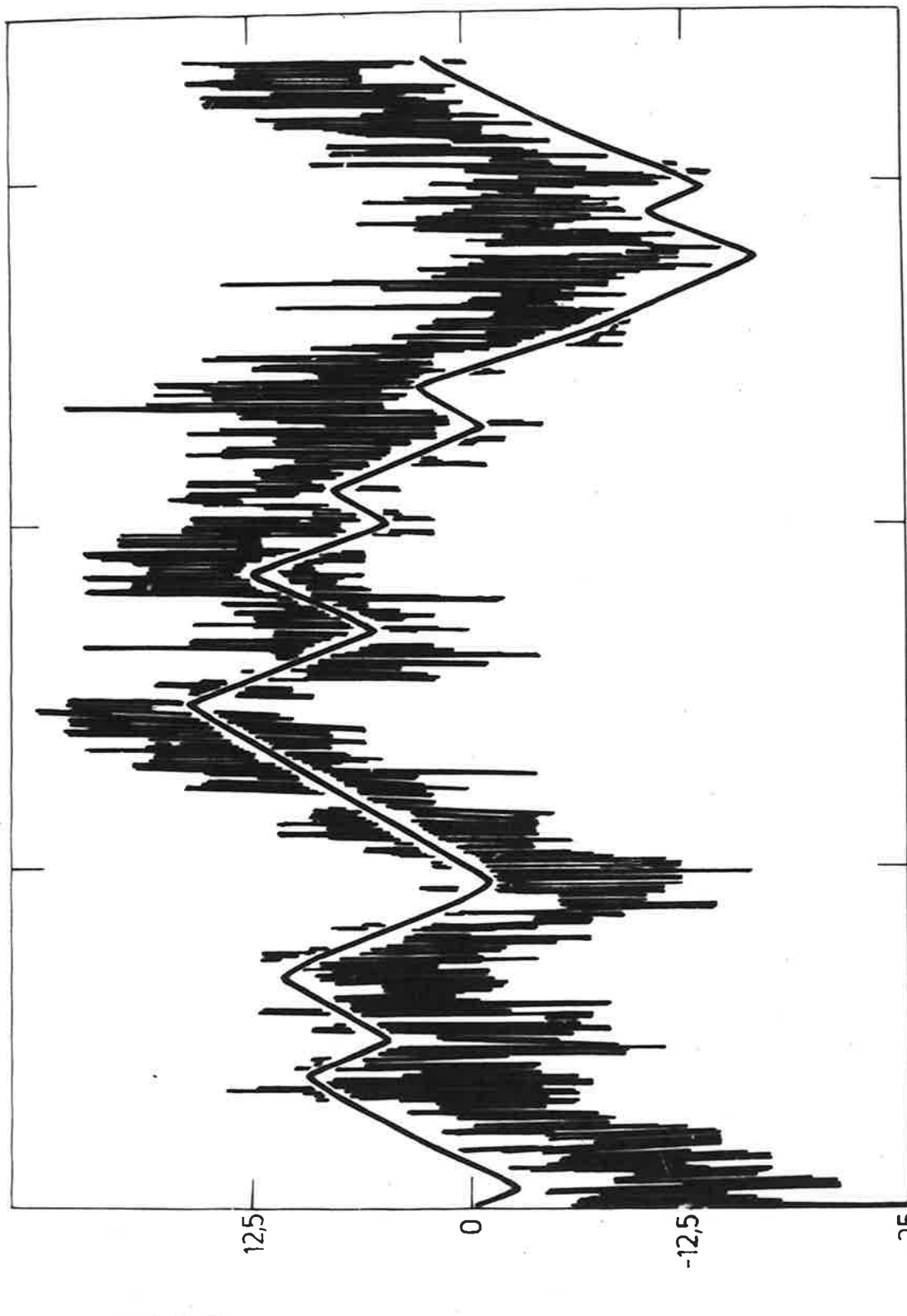

Fig. 26 Comparison between the measured output (with higher frequences) and the deterministic model output for the exp. No. 2

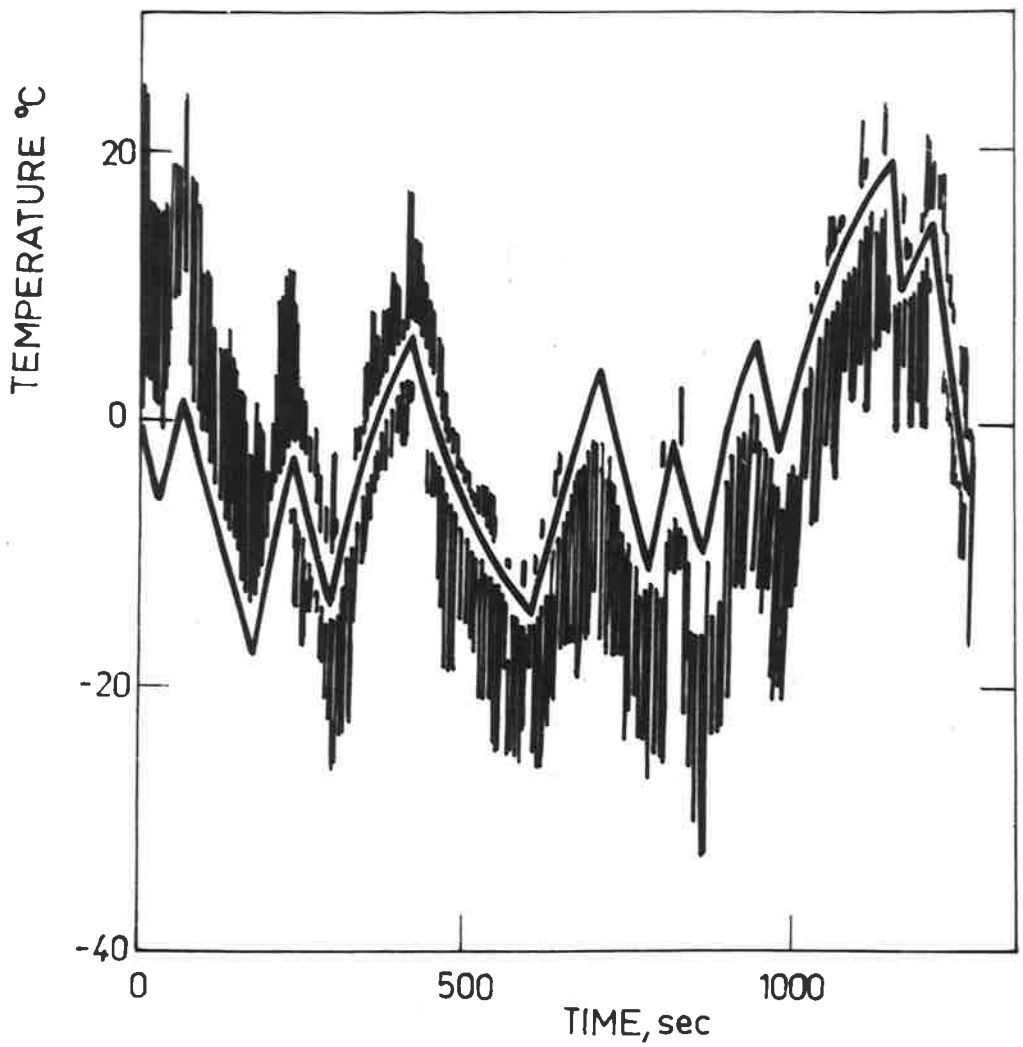

Fig. 27 Comparison between the mea sured output (with higher frequences) and the deterministic model output for the exp. No. 3

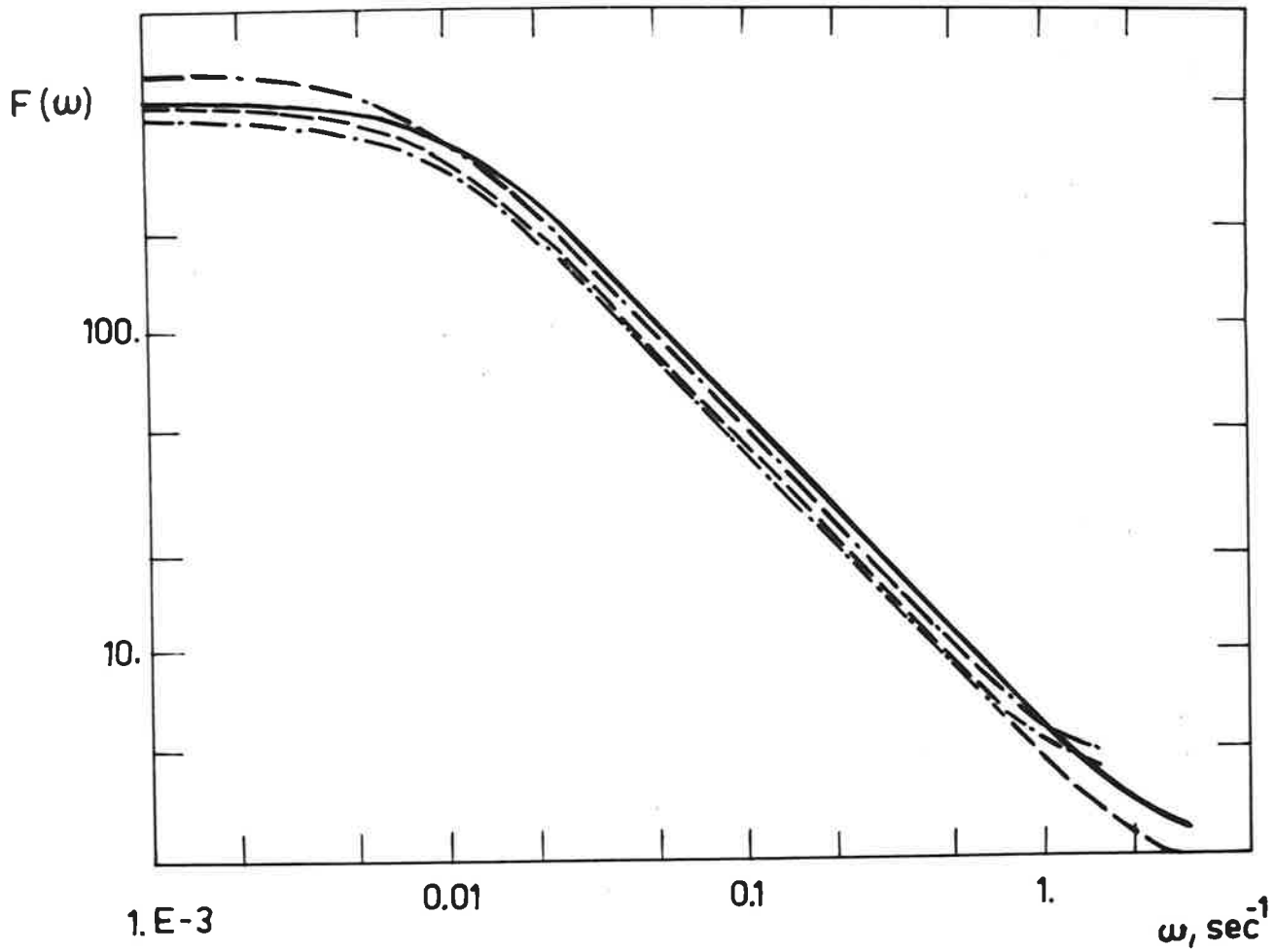

Fig. 28 Comparison between the gains of the frequency response functions for the exp. No. 1-4. Exp. No. 1 ——— , No. 2 - - - - , No. 3 - . - . - , No. 4 - - . - -

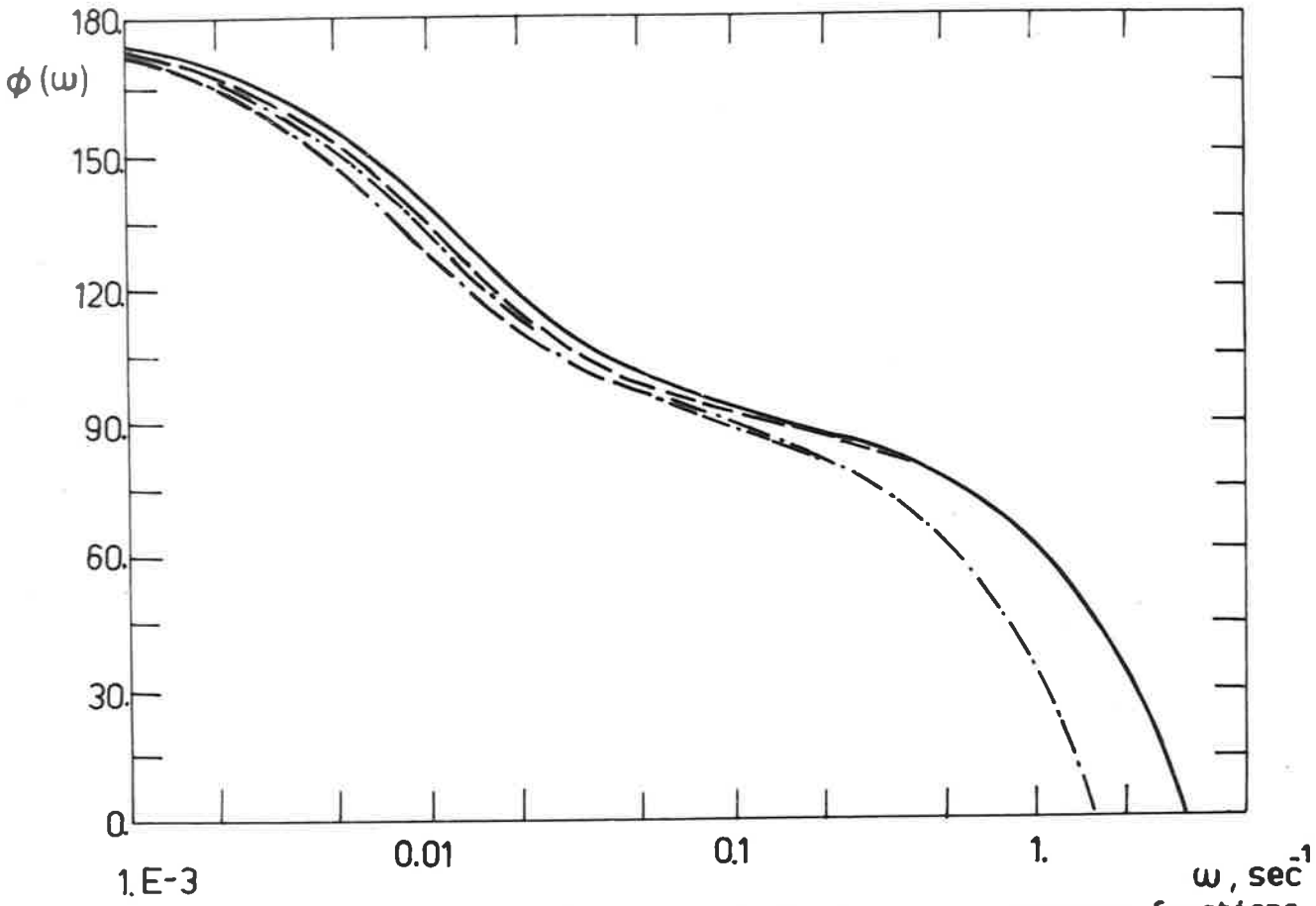

Fig. 29 Comparison between the phase of the frequency response functions for the exp. No. 1-4. Exp. No. 1 ——— , No. 2 - - - - , No. 3 - . - . - . - , No. 4 - - . - - .

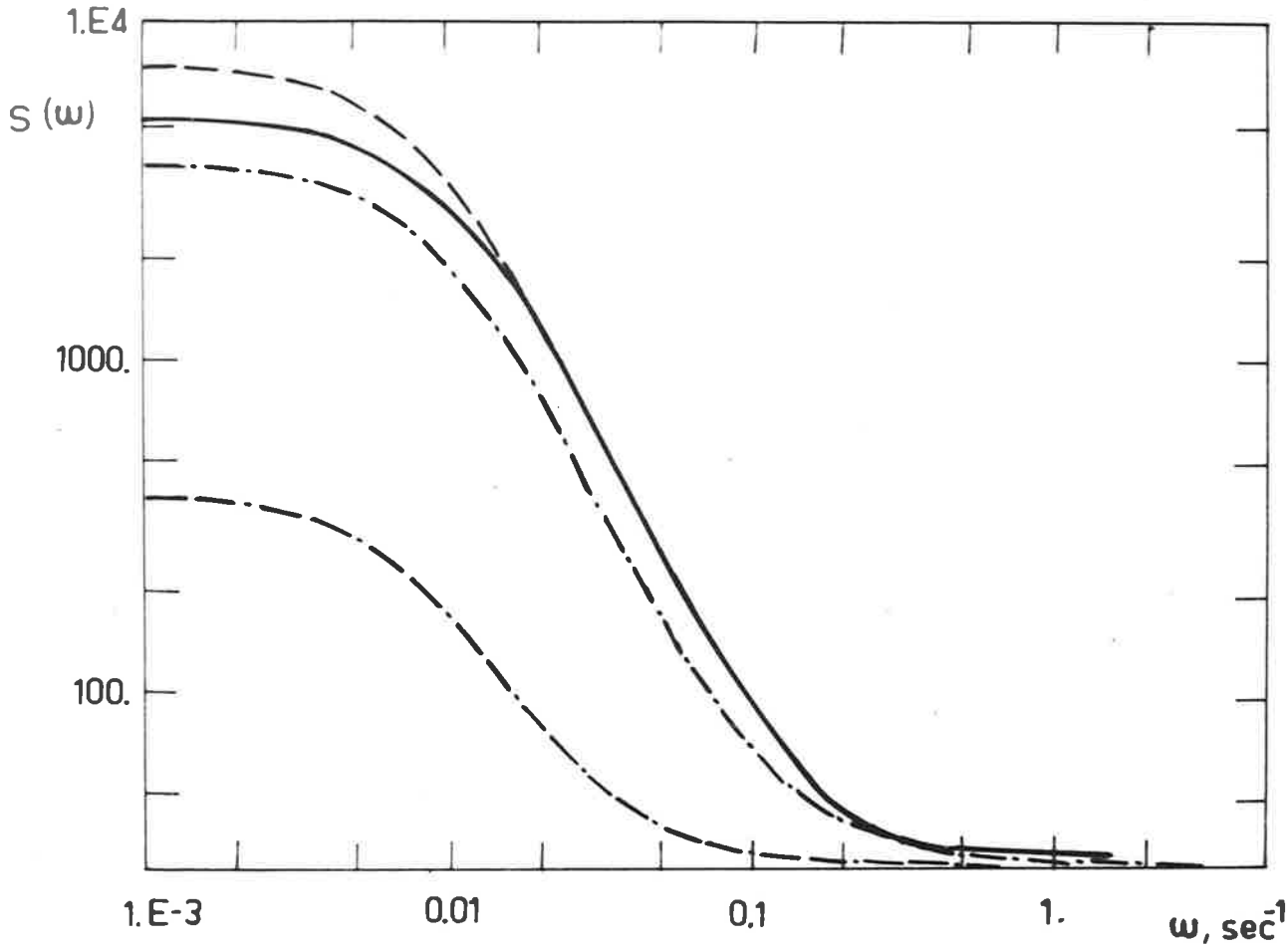

Fig. 30 Comparison between the power spectra of the disturbances for the exp. No. 1-4. Exp. No. 1 ——— , No. 2 - - - - , No. 3 - . - . - . - , No. 4 - - , - - .